Topic 2G - Molecular Orbital Theory

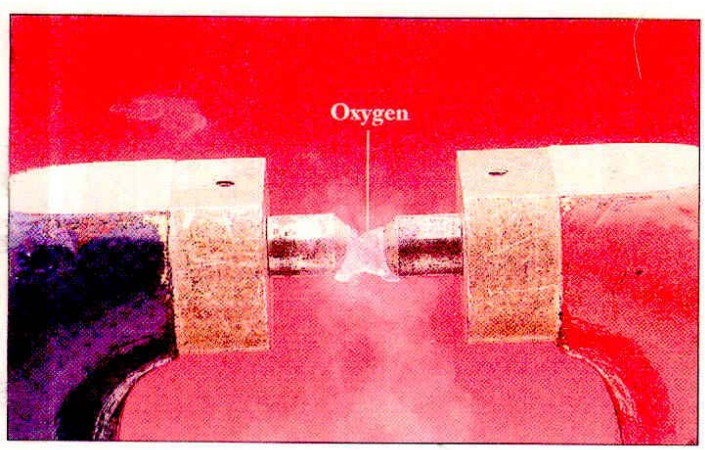

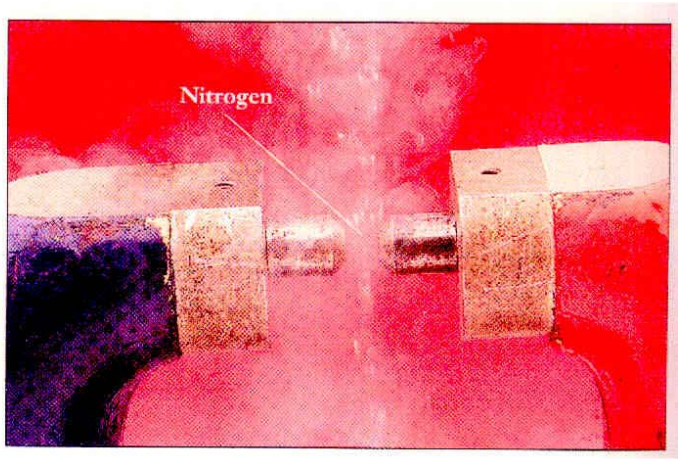

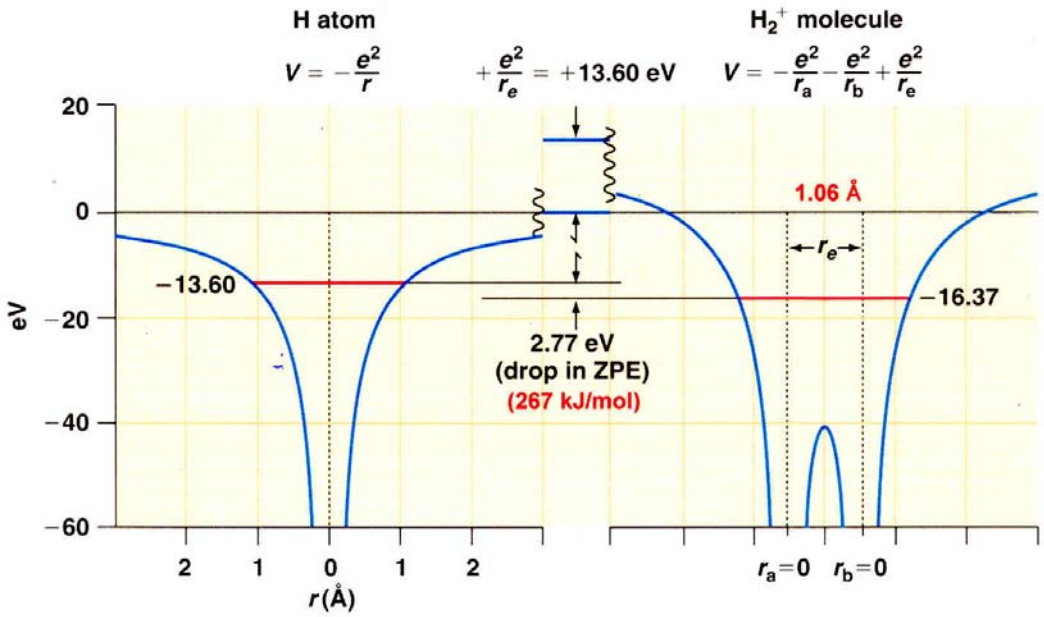

Figure 7.4
Two-dimensional Coulomb potential energies for an electron in the field of a single proton (H atom) and of two protons at fixed distance $r = r_e$ (H_2^+ molecule). In the molecule case the plot gives the potential energy along the bond axis, adjusted for proton–proton repulsion as indicated in the center. The wider Coulomb well for H_2^+ causes the zero point energy (ZPE) to drop and gives rise to bond formation. See Figures 1.10 and 2.12 for details of 2-D potentials and energies in the H atom.

For the H_2^+ molecule $(H_A \cdots H_B)^+$:

$$\psi = C_A \psi^A_{1s} + C_B \psi^B_{1s}$$

where $C_A = \pm C_B$ (since the two nuclei are identical).

Molecular orbitals may thus be constructed as follows:

$$\sigma_{1s} = C_1 [\psi^A_{1s} + \psi^B_{1s}]$$

$$\sigma^*_{1s} = C_2 [\psi^A_{1s} - \psi^B_{1s}]$$

The distribution of electron density probability is obtained from the square of the wave function:

$$(\sigma_{1s})^2 = C_1^2 [(\psi^A_{1s})^2 + 2\psi^A_{1s}\psi^B_{1s} + (\psi^B_{1s})^2]$$

$$(\sigma^*_{1s})^2 = C_2^2 [(\psi^A_{1s})^2 - 2\psi^A_{1s}\psi^B_{1s} + (\psi^B_{1s})^2]$$

For a non-interacting system (*i.e.*, no overlap of ψ^A_{1s} and ψ^B_{1s}:

$$\psi^2 \text{ (n.i.)} = C_3^2 [(\psi^A_{1s})^2 + (\psi^B_{1s})^2]$$

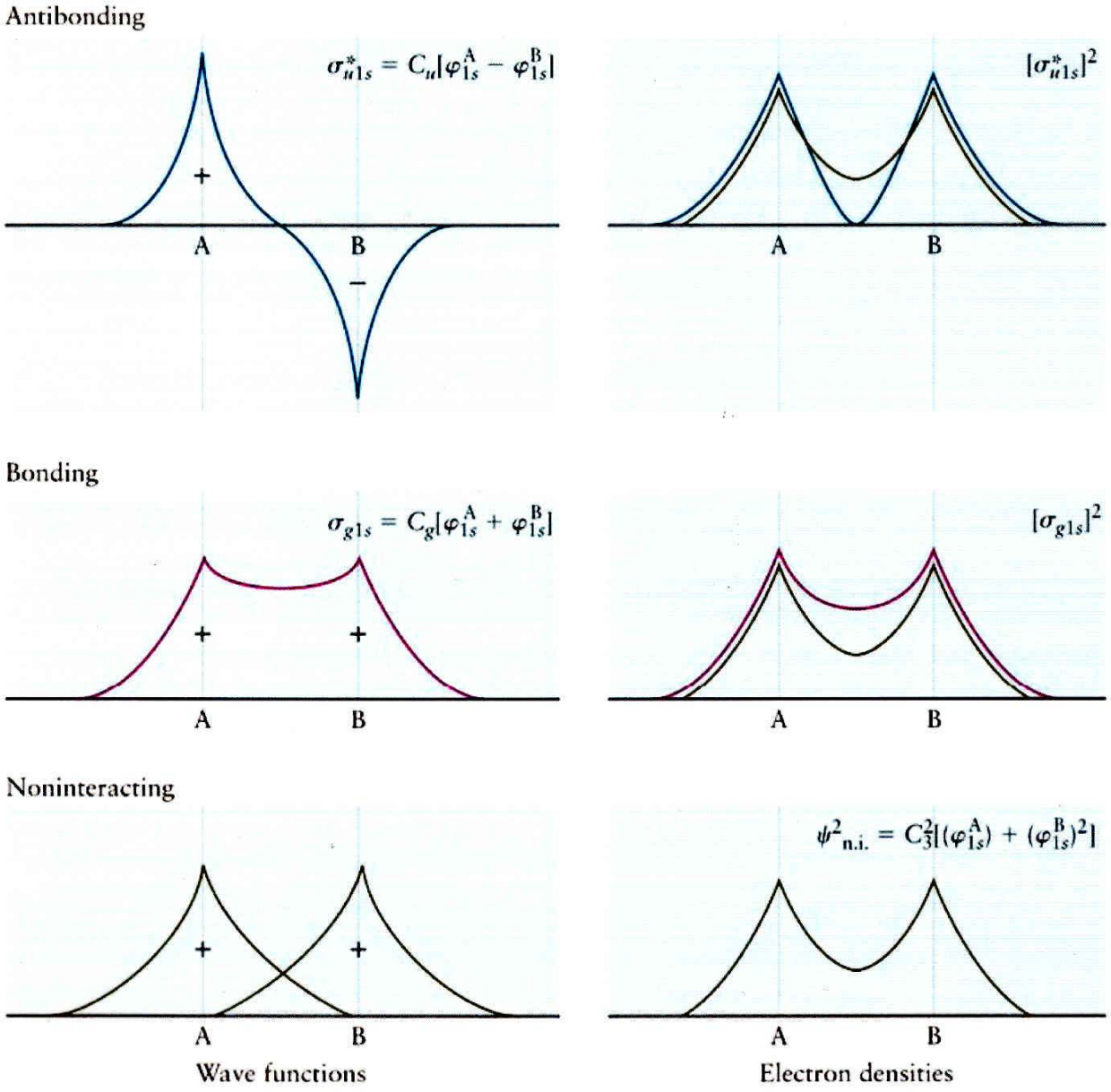

FIGURE 6.6 Antibonding and bonding molecular orbitals of H_2^+ along the internuclear axis in the linear combination of atomic orbitals (LCAO) approximation. For comparison, the green lines show the independent atomic orbitals and the electron probability distribution ψ^2(n.i.) for a noninteracting system. Compared with this reference system, the bonding orbital shows *increased* probability density between the nuclei, but the antibonding orbital shows *decreased* probability density in this region.

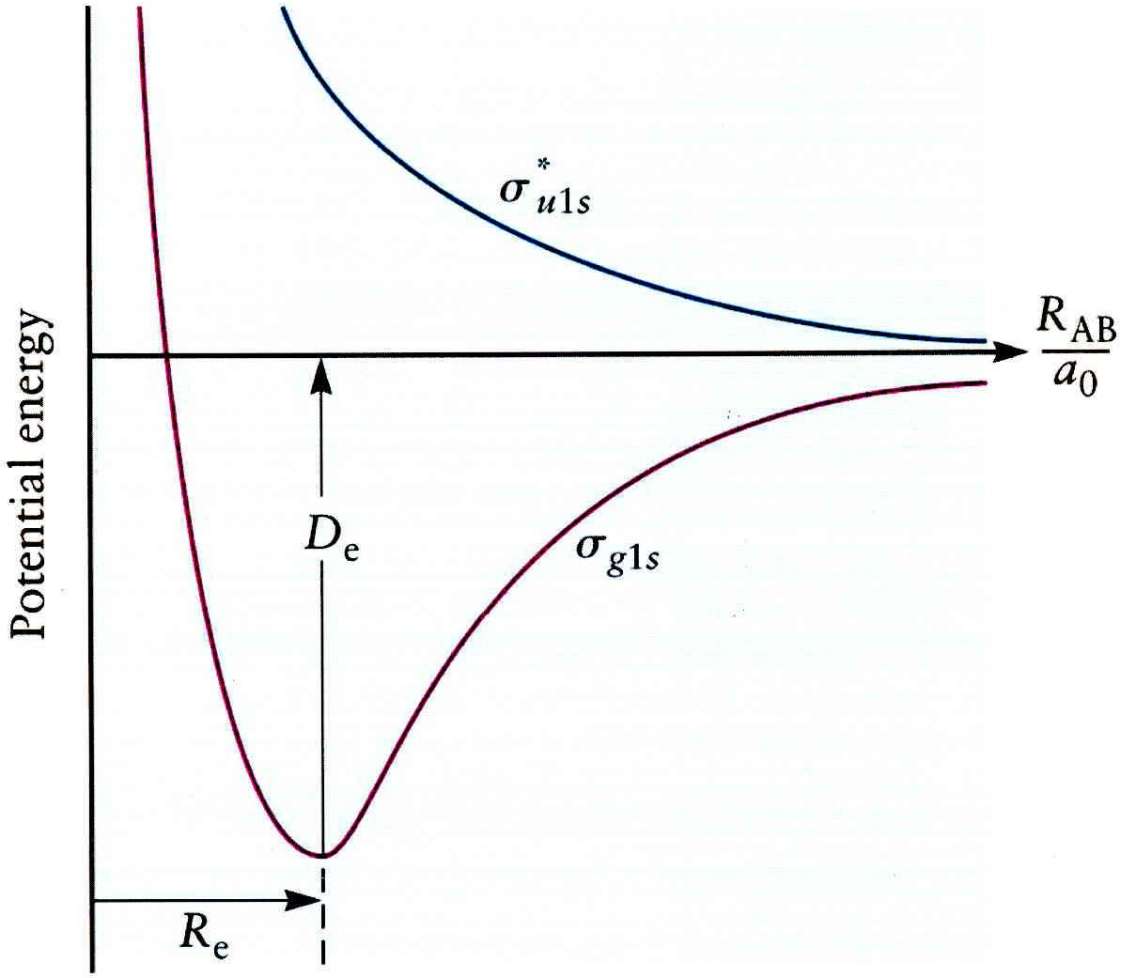

FIGURE 6.7 Potential energy of H_2^+ in a σ_{g1s} (bonding) and σ^*_{u1s} (antibonding) molecular orbital, shown as a function of internuclear separation R_{AB} in the LCAO approximation.

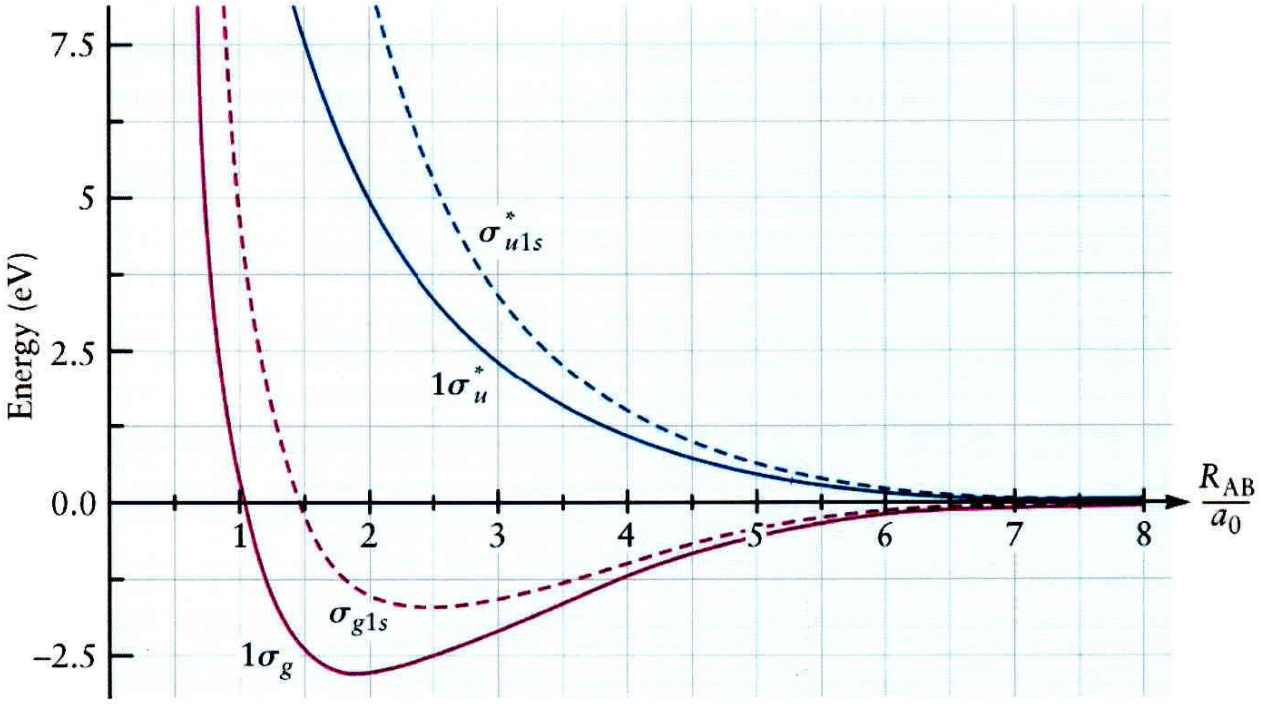

FIGURE 6.8 Comparison of potential energy for the σ_{g1s} and σ^*_{u1s} orbitals of H_2^+ in the LCAO approximation (dashed lines) with the exact results (solid lines). The internuclear separation is plotted in units of the Bohr radius.

FIGURE 6.9 Correlation diagram for H_2^+ in the linear combination of atomic orbitals (LCAO) approximation. The bonding orbital is stabilized relative to the noninteracting system by the energy difference ΔE.

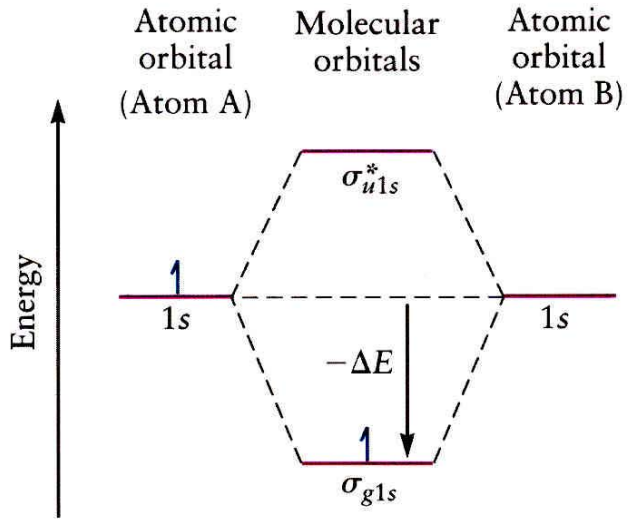

Figure 7.2: Potential Energy Curves (H_2^+)

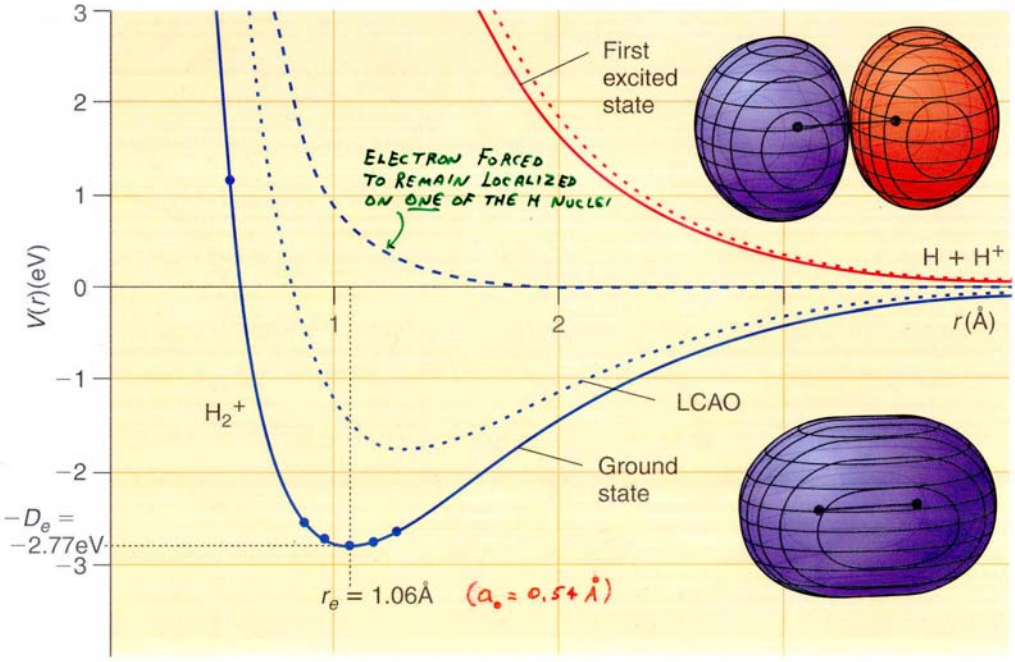

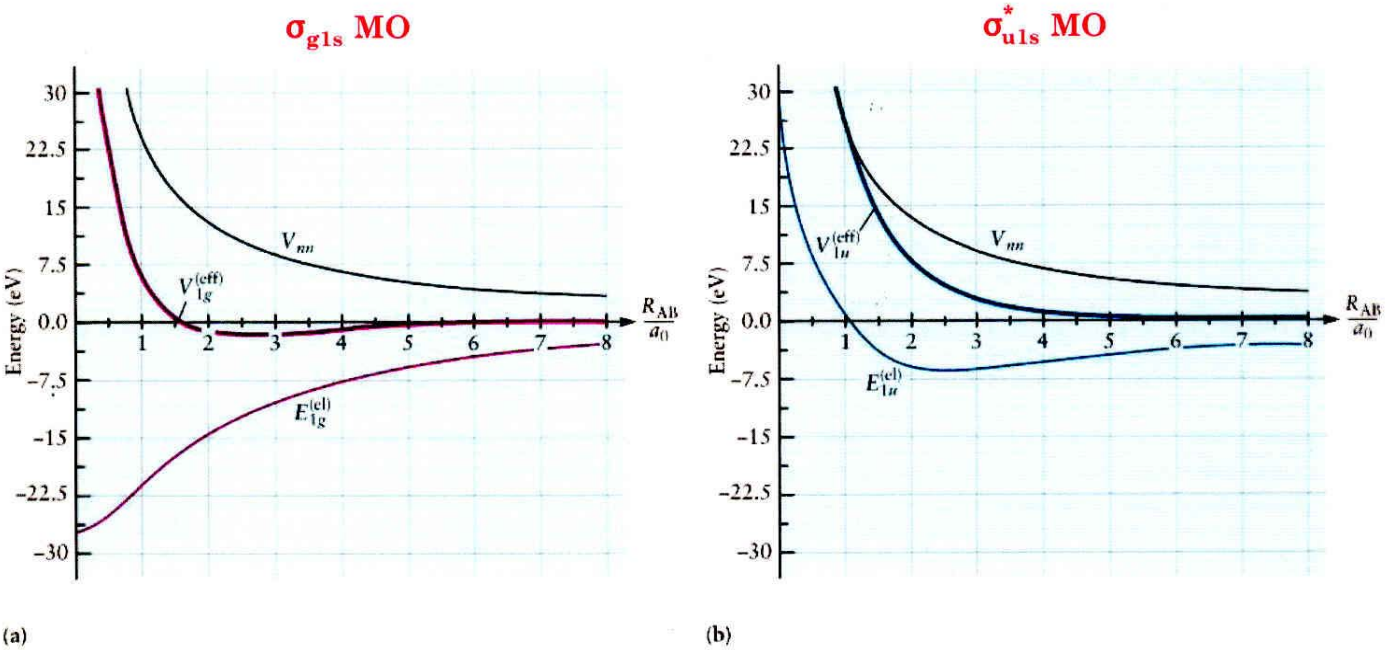

FIGURE 6.22 Dependence on internuclear distance of the contributions to the effective potential energy of the nuclei in H_2^+. (a) The effective potential energy in the σ_{g1s} MO. The electronic bonding energy for the electron is the lighter red curve, the internuclear repulsion between the protons is the black curve, and their sum is the heavier red curve. (b) The effective potential energy in the σ^*_{u1s} MO. The electronic bonding energy for the electron is the lighter blue curve, the internuclear repulsion between the protons is the black curve, and their sum is the heavier blue curve. The behavior of the effective potential energy shows that the σ_{g1s} MO is bonding and that the σ^*_{u1s} MO is antibonding.

FIGURE 6.10 Correlation diagram for first-period diatomic molecules. Blue arrows indicate the electron filling for the H_2 molecule. All of the atomic electrons are pooled and used to fill the molecular orbitals using the aufbau principle. In the molecules, electrons are no longer connected to any particular atom.

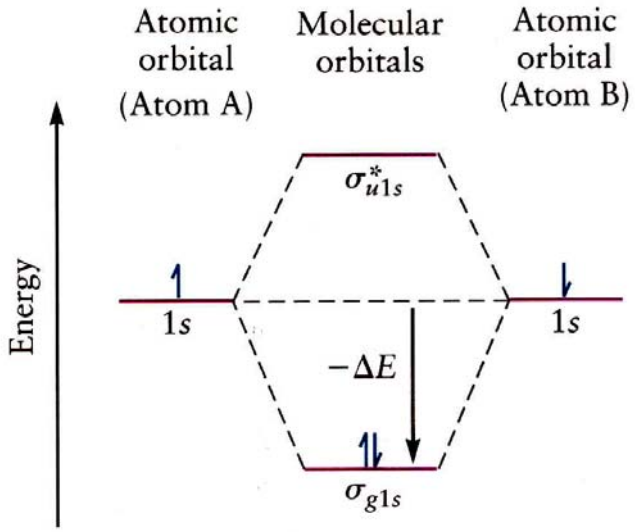

FIGURE 6.11 Correlation diagram for first-period diatomic molecules. Blue arrows indicate the electron filling for the He_2^+ molecule. The aufbau principle fills the bonding orbital with two electrons, so the third electron must go into the antibonding orbital, thus reducing the bond order compared with that in H_2.

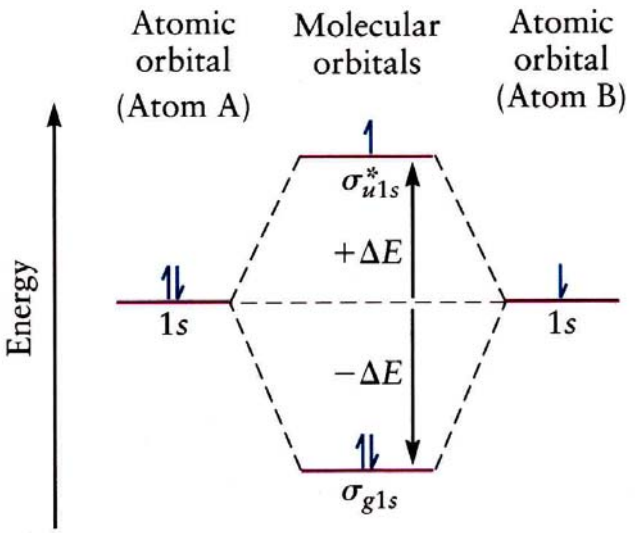

TABLE 6.2 Electron Configurations and Bond Orders for First-Row Diatomic Molecules

Species	Electron Configuration	Bond Order	Bond Energy (kJ mol^{-1})	Bond Length (Å)
H_2^+	$(\sigma_{g1s})^1$	$\frac{1}{2}$	255	1.06
H_2	$(\sigma_{g1s})^2$	1	431	0.74
He_2^+	$(\sigma_{g1s})^2(\sigma^*_{u1s})^1$	$\frac{1}{2}$	251	1.08
He_2	$(\sigma_{g1s})^2(\sigma^*_{u1s})^2$	0	~0	Large
H_2^-	$(\sigma_{g1s})^2(\sigma^*_{u1s})^1$	½	----	----

Bond Order = ½ (# of e⁻'s in Bonding MO's - # of e⁻'s in Anti-Bonding MO's)

Molecular Orbital Description of Bonding

1.) Form Linear Combinations of Atomic Orbitals (LCAO's) to give Molecular Orbitals (M.O.'s).

Total No. of M.O.'s Formed = No. of A.O.'s Used

2.) Place M.O.'s in order, from lowest to highest energy.

3.) Electrons occupy M.O.'s in pairs (with opposite spins), starting with lowest energy M.O. Hund's rules apply, where appropriate.

4.) Average energy of bonding-antibonding M.O. pair ≈ energy of original A.O.'s.

5.) ΔE between bonding-antibonding M.O. pair increases with increasing overlap of A.O.'s.

6.) Two AO's on different atoms contribute to bond formation only if their energy levels are close to one another.

7.) Two AO's on different atoms contribute to bond formation only if they overlap significantly.

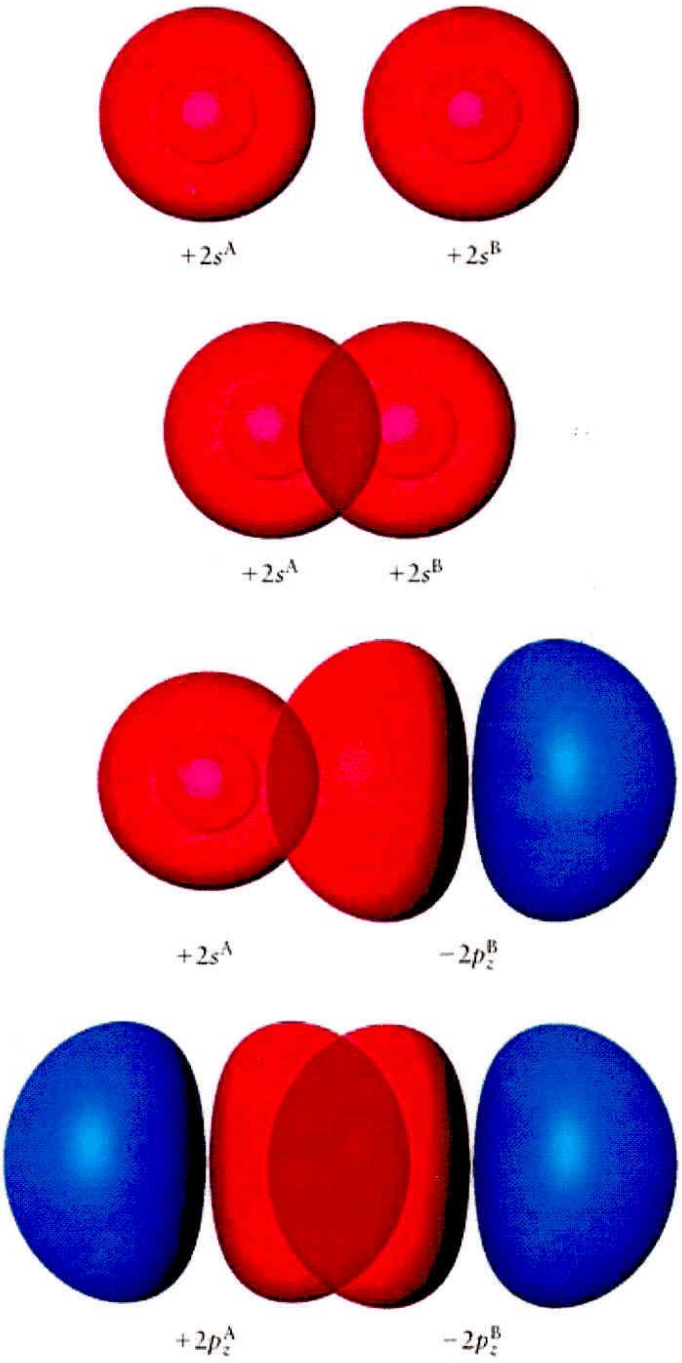

FIGURE 6.12 Overlap of orbitals in several common combinations. The magnitude of overlap can be estimated qualitatively from the relative size and symmetry of the two orbitals involved. (Note the radial nodes in the 2*s* orbitals, clearly visible in these images.)

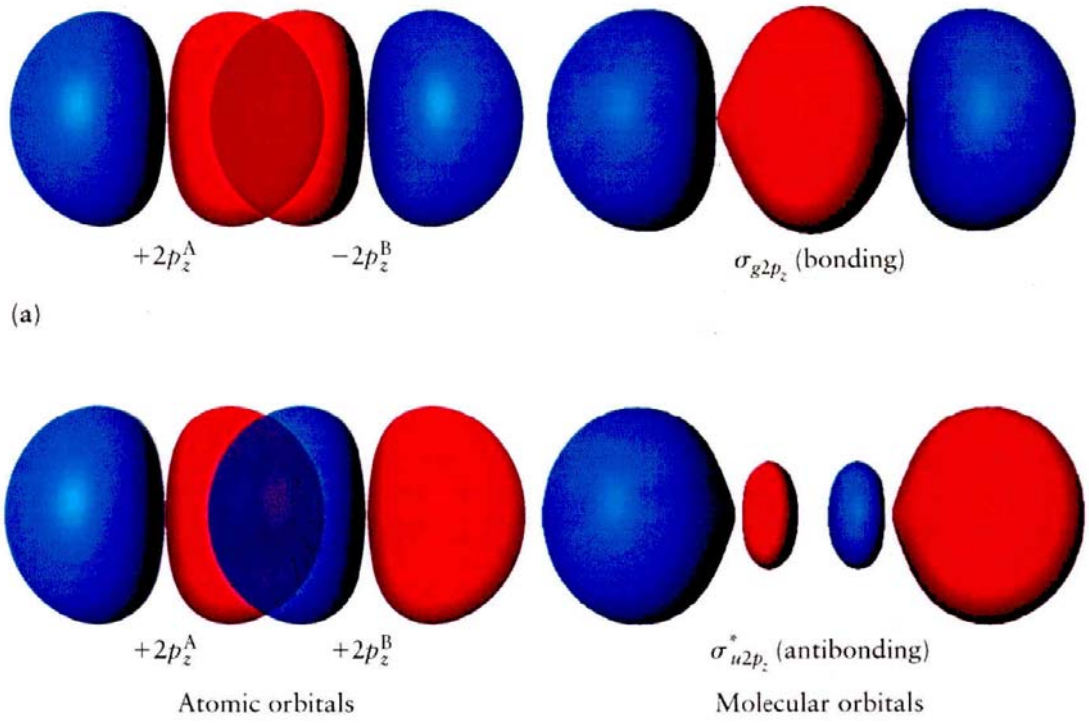

FIGURE 6.13 Formation of (a) σ_{g2p_z} bonding and (b) $\sigma^*_{u2p_z}$ antibonding molecular orbitals from $2p_z$ orbitals on atoms A and B. Regions with positive amplitude are shown in red, and those with negative amplitude are shown in blue.

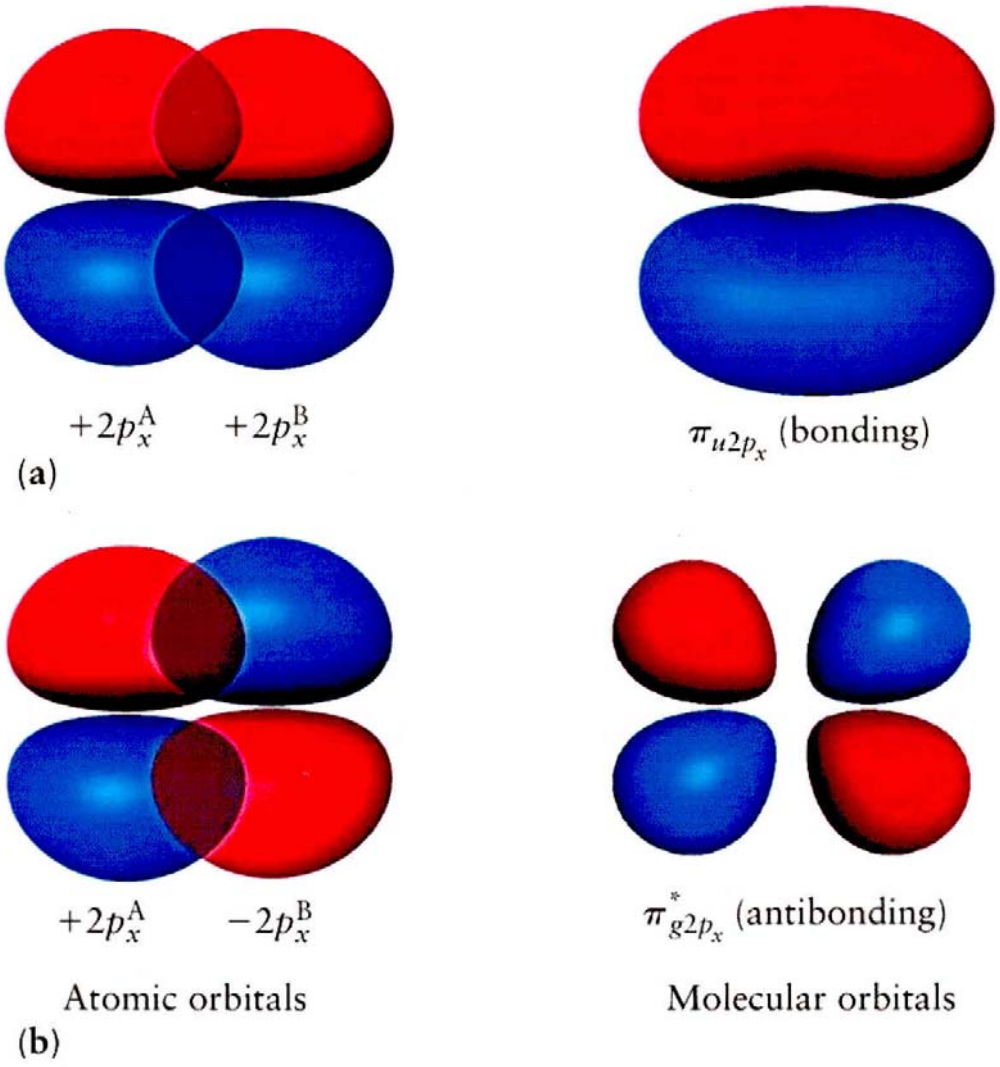

FIGURE 6.14 Formation of (a) π_{u2p_x} bonding and (b) $\pi^*_{g2p_x}$ antibonding molecular orbitals from $2p_x$ orbitals on atoms A and B.

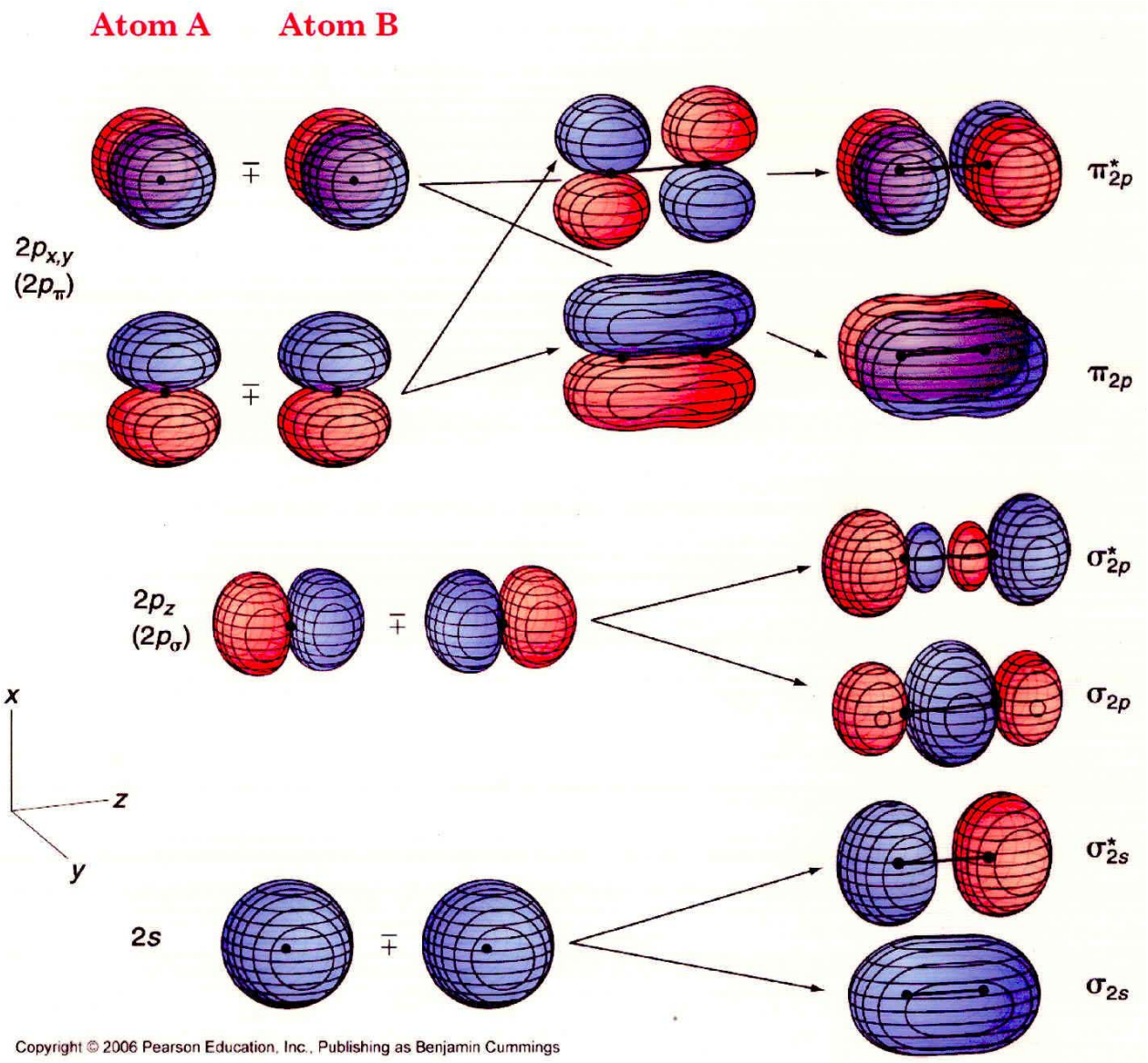

Copyright © 2006 Pearson Education, Inc., Publishing as Benjamin Cummings

Figure 7.6
LCAO-MOs for the $n = 2$ valence shell homonuclear diatomic molecules. Each pair of atomic orbitals gives a bonding and antibonding MO. Note the nodes midway between the nuclei (heavy dots) for the antibonding orbitals (i.e., those denoted by an asterisk). Similar boundary surfaces are obtained for the later periods.

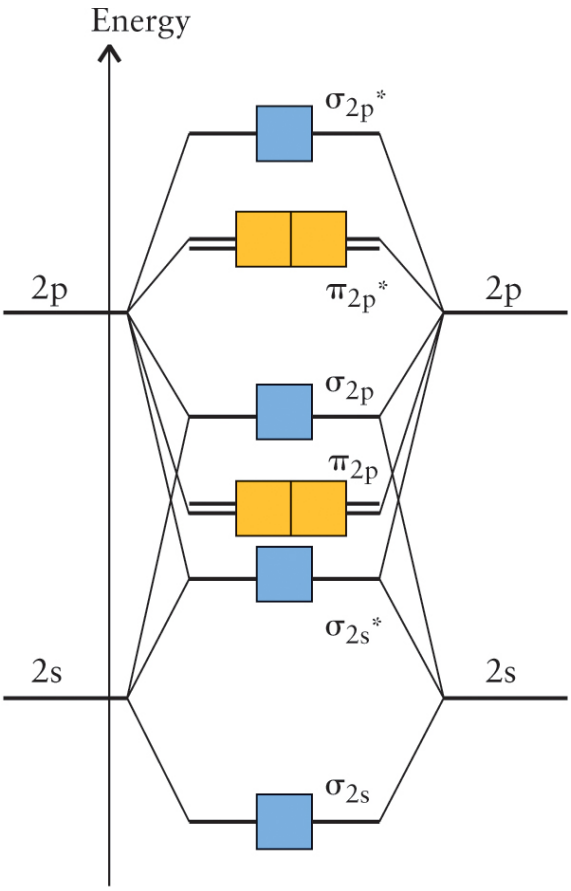

FIGURE 4.31 A typical molecular orbital energy-level diagram for the homonuclear diatomic molecules Li_2 through N_2. Each box represents one molecular orbital and can accommodate up to two electrons.

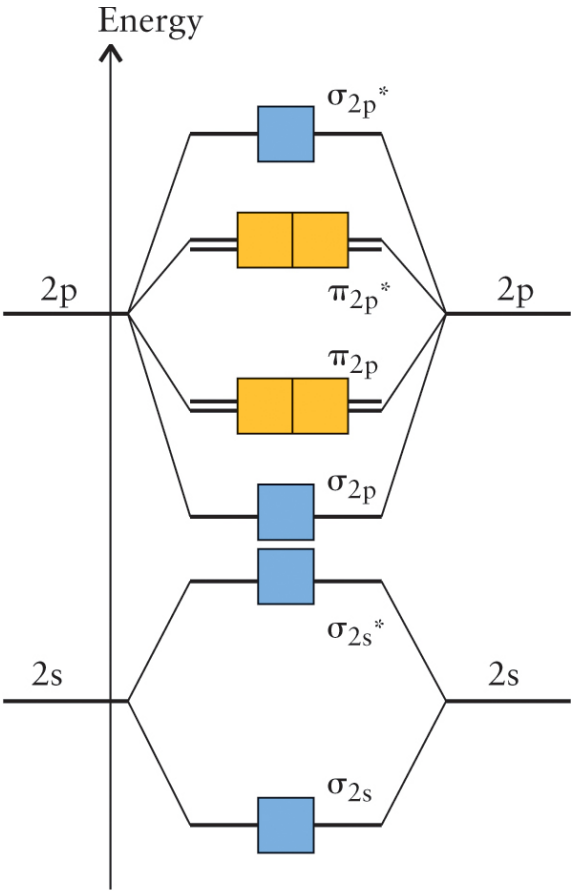

FIGURE 4.32 The molecular orbital energy-level diagram for the homonuclear diatomic molecules on the right-hand side of Period 2, specifically O_2 and F_2.

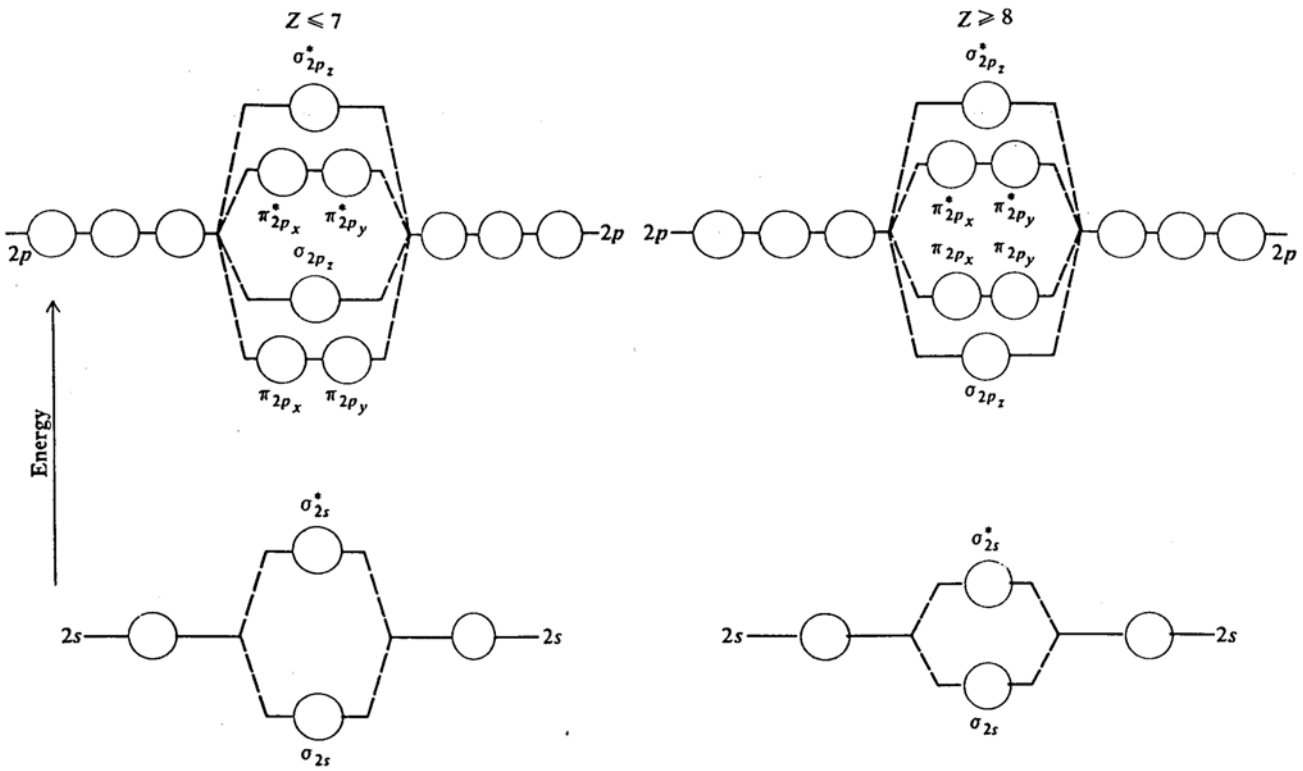

Correlation diagrams for second-period diatomic molecules. In each case, the atomic orbitals at the sides combine to give the molecular orbitals in the center.

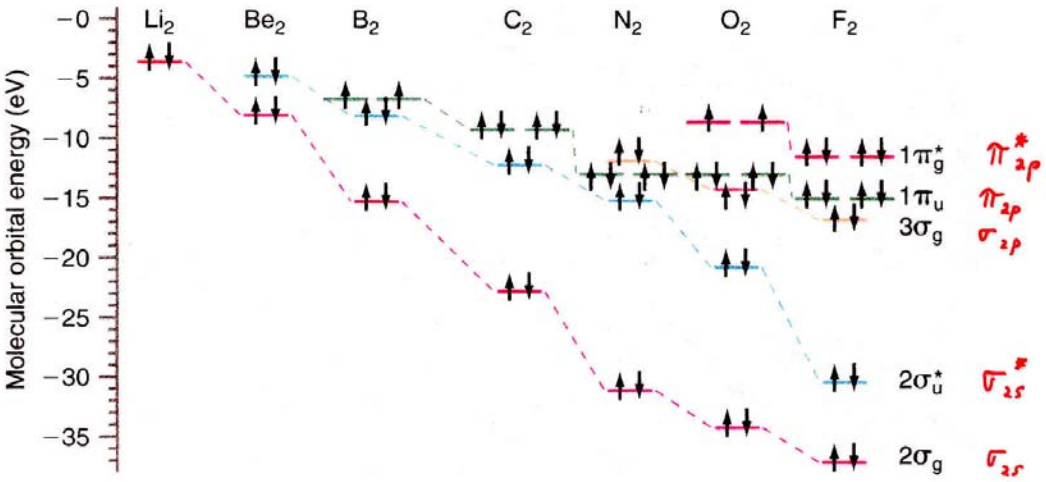

FIGURE 23.18

Molecular orbital energy levels for occupied MOs of the second row diatomics. The $1\sigma_g$ and $1\sigma_u^*$ orbitals lie at much lower values of energy and are not shown.

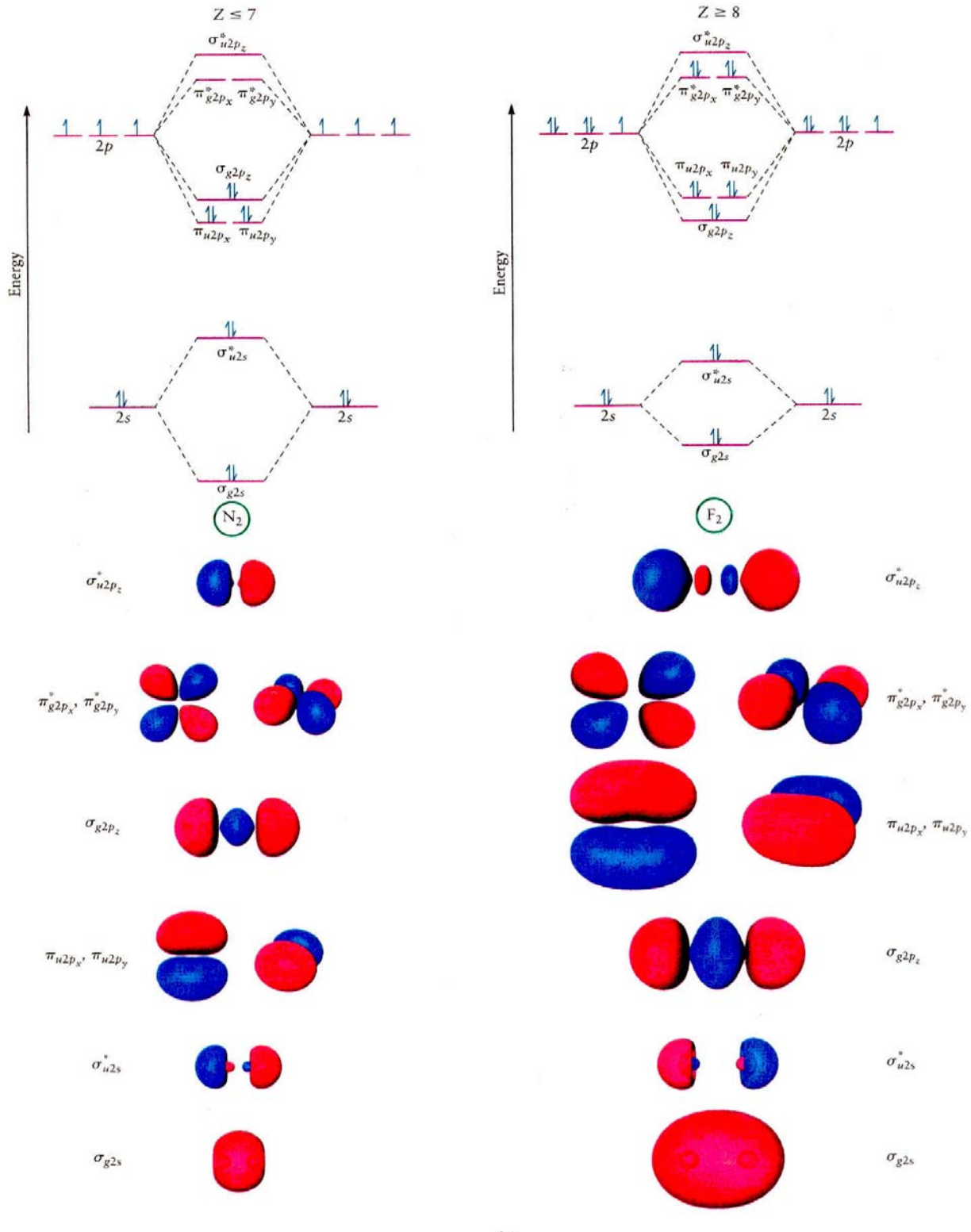

FIGURE 6.16 Correlation diagrams for second-period diatomic molecules. (a) Correlation diagram and molecular orbitals calculated for N_2. (b) Correlation diagram and molecular orbitals calculated for F_2.

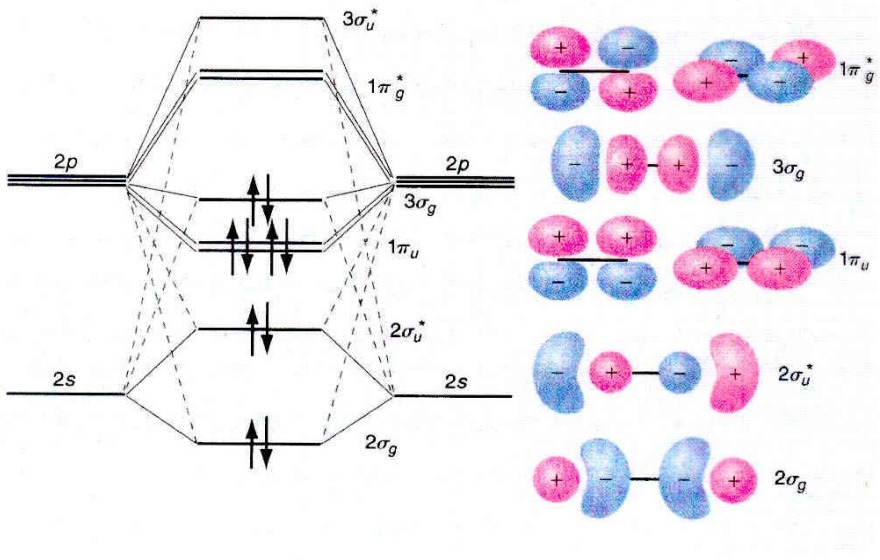

FIGURE 23.17

Schematic MO energy diagram for the valence electrons in N_2. The degenerate p and π orbitals are shown slightly offset in energy. The dominant AO contributions to the MOs are shown as solid lines. Lesser contributions arising from $s-p$ mixing are shown as dashed lines. The MOs are schematically depicted to the right of the figure. The $1\sigma_g$ and $1\sigma_u^*$ MOs are not shown.

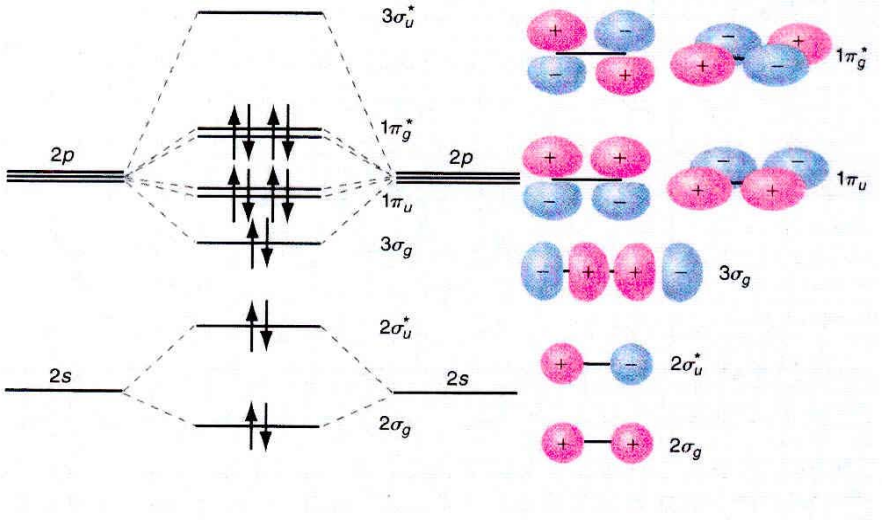

FIGURE 23.16

Schematic MO energy diagram for the valence electrons in F_2. The degenerate p and π orbitals are shown slightly offset in energy. The dominant atomic orbital contributions to the MOs are shown as solid lines. Minor contributions due to $s-p$ mixing have been neglected. The MOs are schematically depicted to the right of the figure. The $1\sigma_g$ and $1\sigma_u^*$ MOs are not shown.

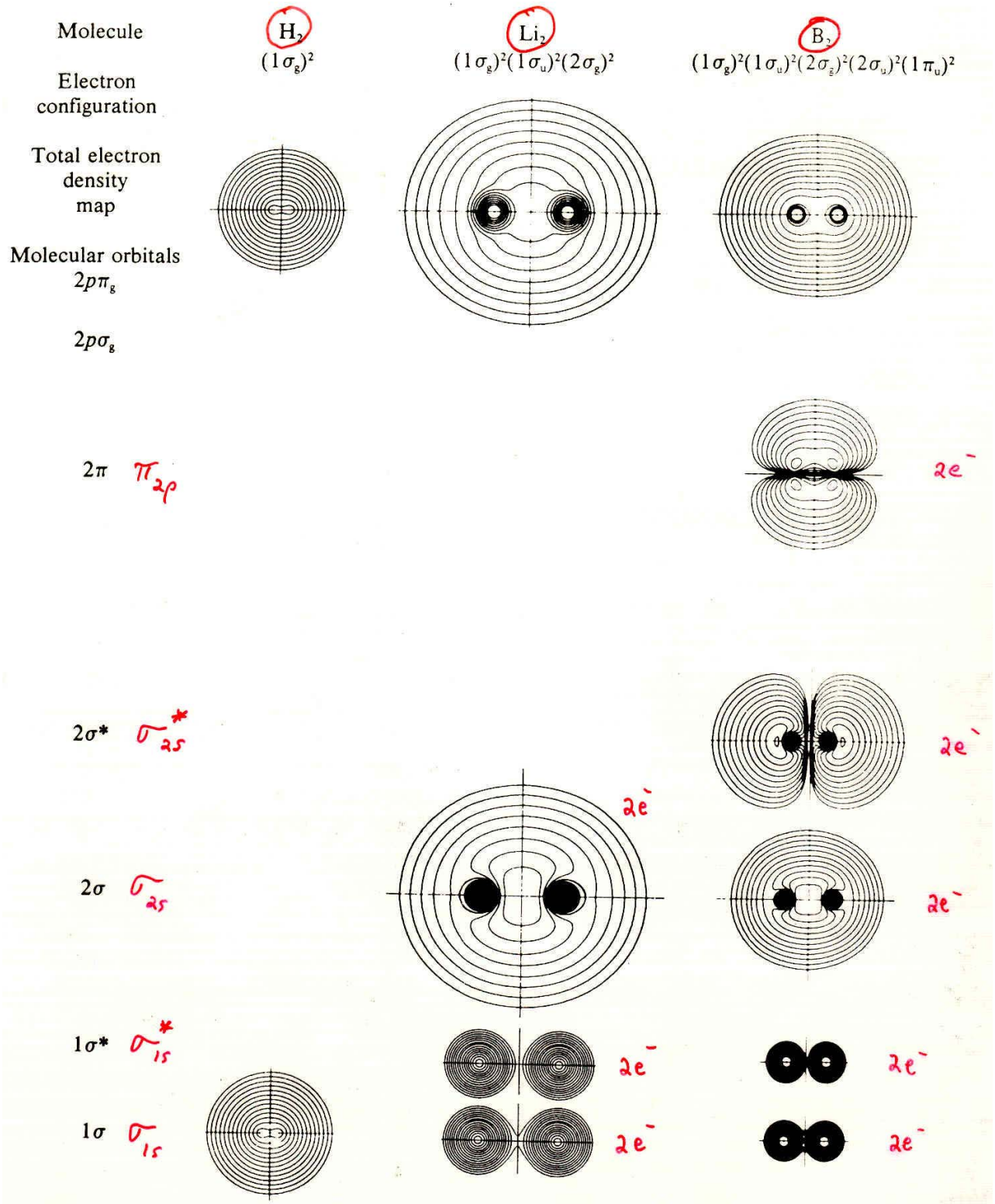

FIGURE 9.20
Contour maps of the various molecular orbitals and the total electron density of the homonuclear diatomic molecules H_2 through F_2.

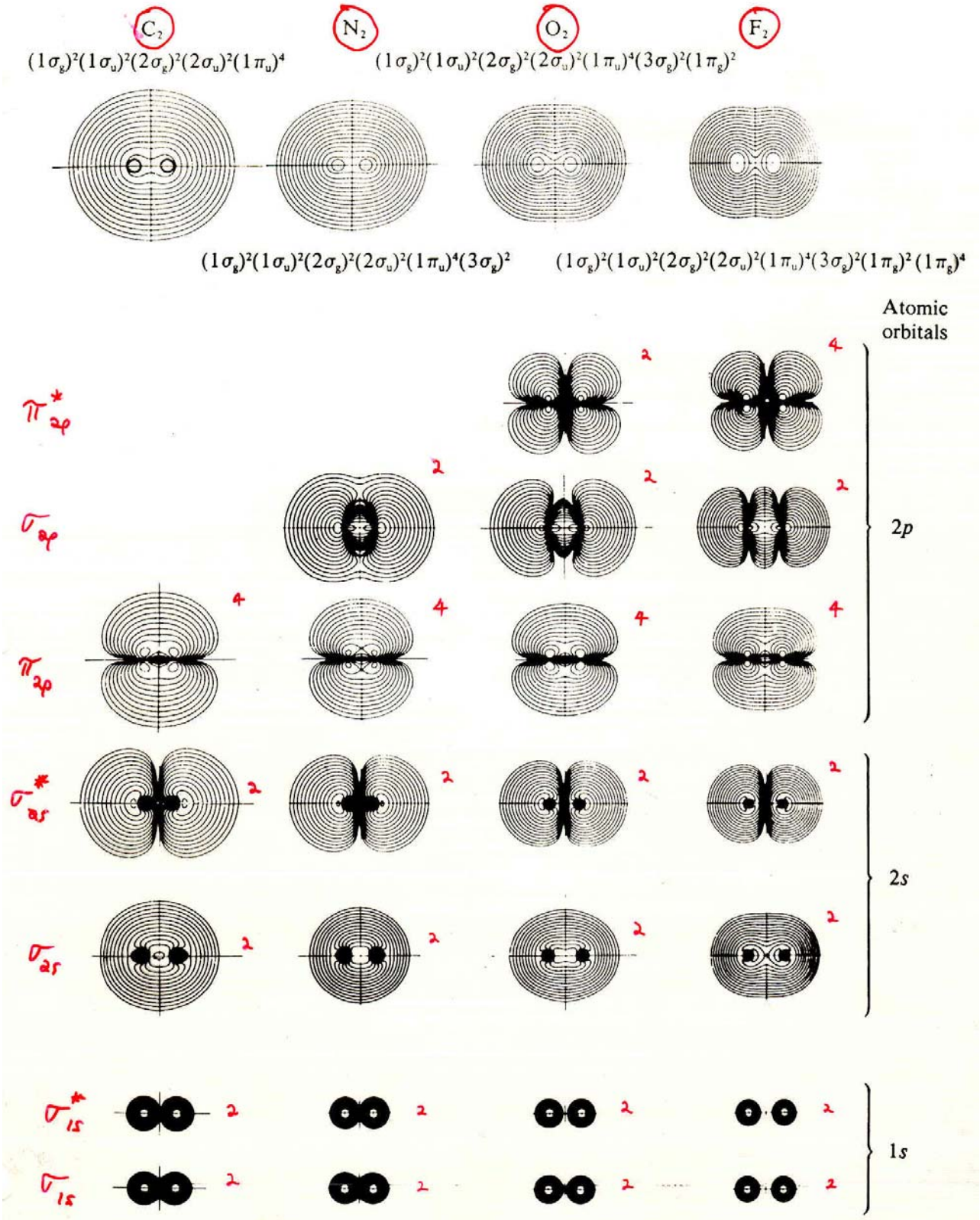
C2
N2
O2
F2
(1σg)²(1σu)²(2σg)²(2σu)²(1πu)⁴
(1σg)²(1σu)²(2σg)²(2σu)²(1πu)⁴(3σg)²(1πg)²
(1σg)²(1σu)²(2σg)²(2σu)²(1πu)⁴(3σg)²
(1σg)²(1σu)²(2σg)²(2σu)²(1πu)⁴(3σg)²(1πg)²(1πg)⁴
Atomic orbitals
π*2p
σ2p
π2p
σ*2s
σ2s
σ*1s
σ1s
2p
2s
1s

TABLE 6.3 Molecular Orbitals of Homonuclear Diatomic Molecules

Species	Number of Valence Electrons	Valence Electron Configuration	Bond Order	Bond Length (Å)	Bond Energy (kJ mol^{-1})
H_2	2	$(\sigma_{g1s})^2$	1	0.74	431
He_2	4	$(\sigma_{g1s})^2(\sigma^*_{u1s})^2$	0		
Li_2	2	$(\sigma_{g2s})^2$	1	2.67	105
Be_2	4	$(\sigma_{g2s})^2(\sigma^*_{u2s})^2$	0	2.45	9
B_2	6	$(\sigma_{g2s})^2(\sigma^*_{u2s})^2(\pi_{u2p})^2$	1	1.59	289
C_2	8	$(\sigma_{g2s})^2(\sigma^*_{u2s})^2(\pi_{u2p})^4$	2	1.24	599
N_2	10	$(\sigma_{g2s})^2(\sigma^*_{u2s})^2(\pi_{u2p})^4(\sigma_{g2p_z})^2$	3	1.10	942
O_2	12	$(\sigma_{g2s})^2(\sigma^*_{u2s})^2(\sigma_{g2p_z})^2(\pi_{u2p})^4(\pi^*_{g2p})^2$	2	1.21	494
F_2	14	$(\sigma_{g2s})^2(\sigma^*_{u2s})^2(\sigma_{g2p_z})^2(\pi_{u2p})^4(\pi^*_{g2p})^4$	1	1.41	154
Ne_2	16	$(\sigma_{g2s})^2(\sigma^*_{u2s})^2(\sigma_{g2p_z})^2(\pi_{u2p})^4(\pi^*_{g2p})^4(\sigma^*_{u2p_z})^2$	0		

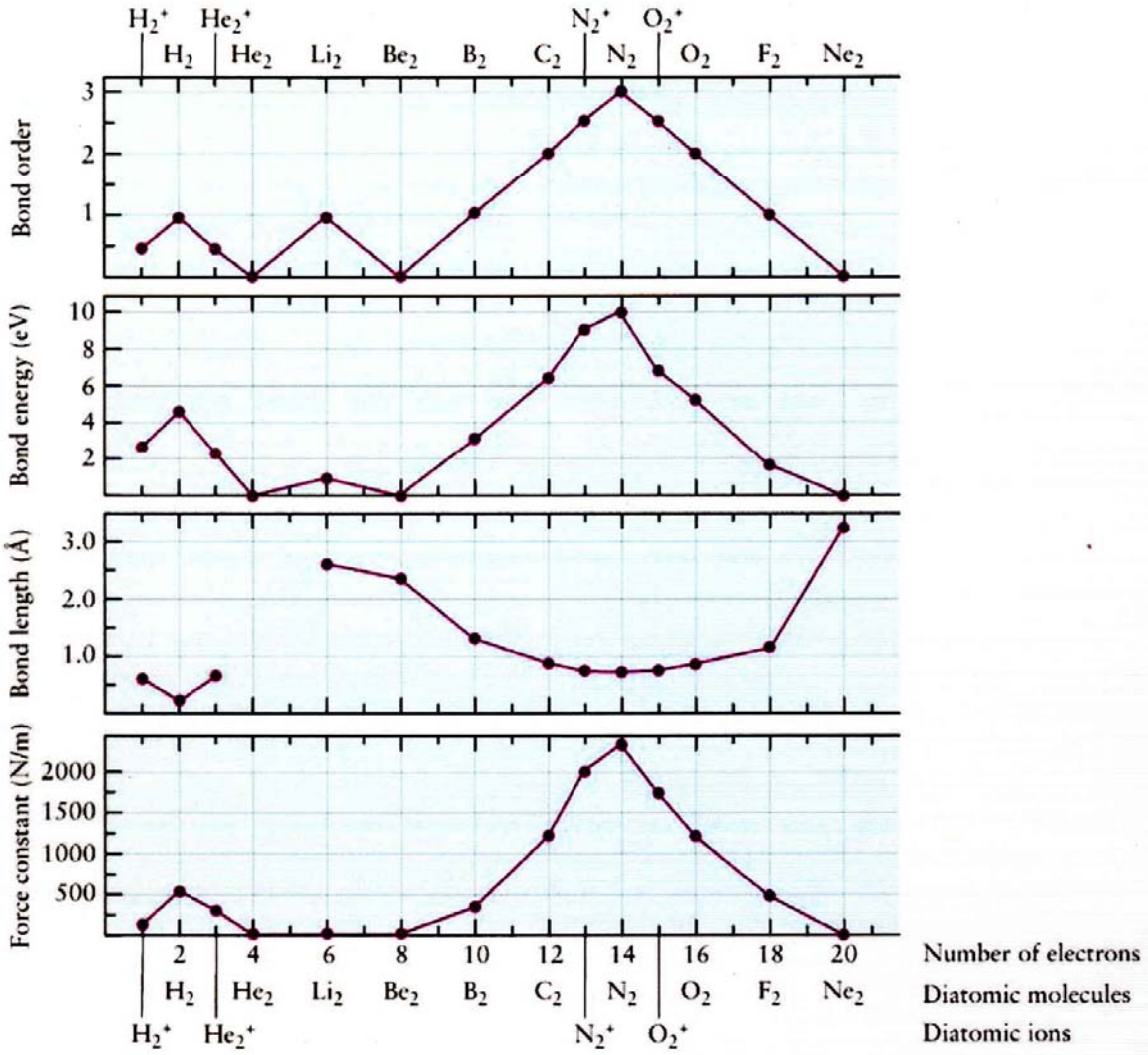

Bonding in Homomolecular Diatomic Molecules

Atom	I.E. (eV)	Molecule	I.E. (eV)	D_e (eV)	r_e (Å)
H	13.60	H_2	15.42	4.75	0.74
He	24.59	He_2	--	--	--
Li	5.39	Li_2	4.96	1.05	2.67
Be	9.32	Be_2	~ 0	0.09	2.45
B	8.30	B_2	12.06	3.00	1.59
C	11.26	C_2	12.00	6.21	1.31
N	14.53	N_2	15.58	9.76	1.10
O	13.62	O_2	12.08	5.12	1.21
F	17.43	F_2	15.70	1.60	1.41
Ne	21.56	Ne_2	--	--	--

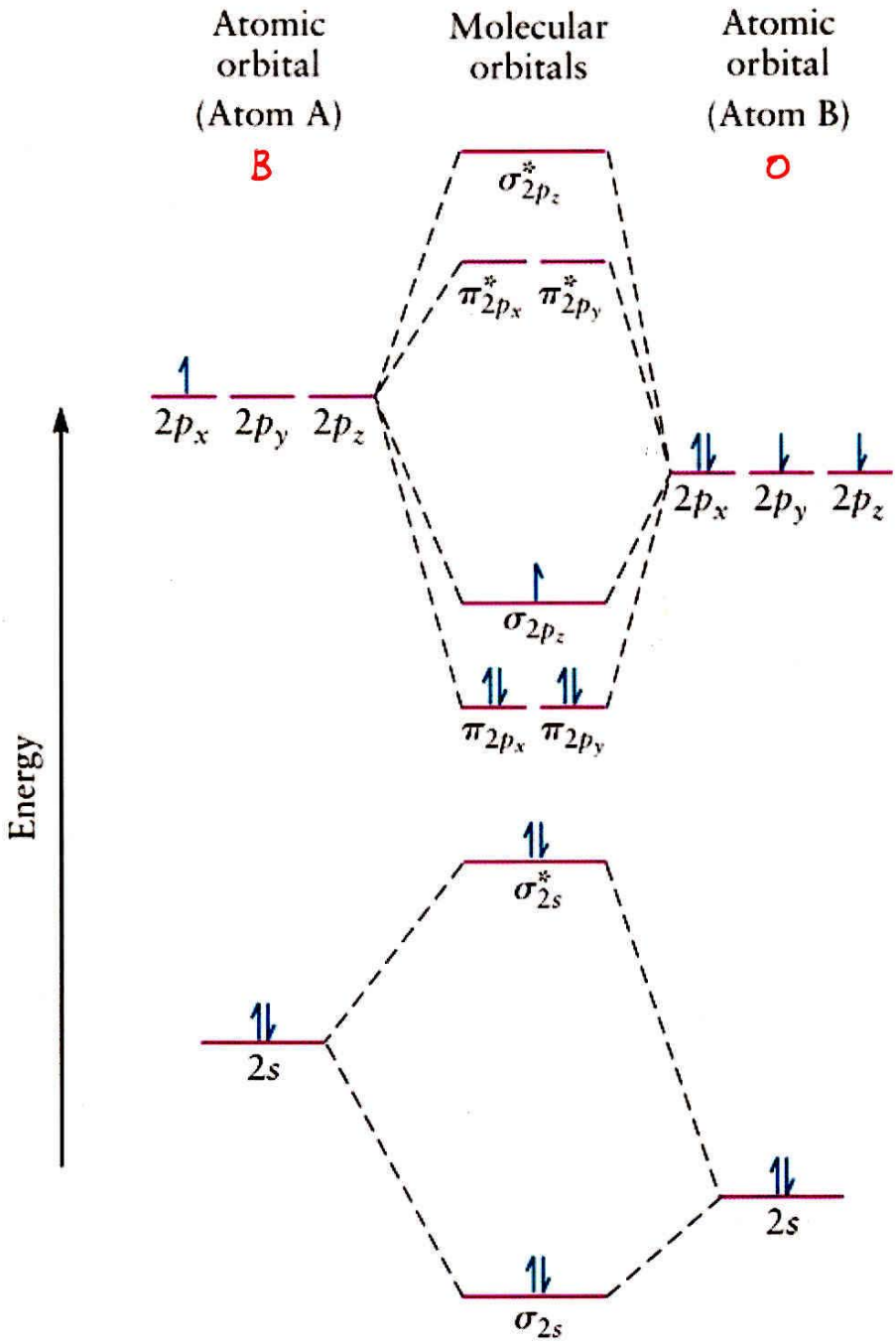

FIGURE 6.19 Correlation diagram for heteronuclear diatomic molecules, AB. The atomic orbitals for the more electronegative atom (B) are displaced downward because they have lower energies than those for A. The orbital filling shown is that for (boron monoxide) BO.

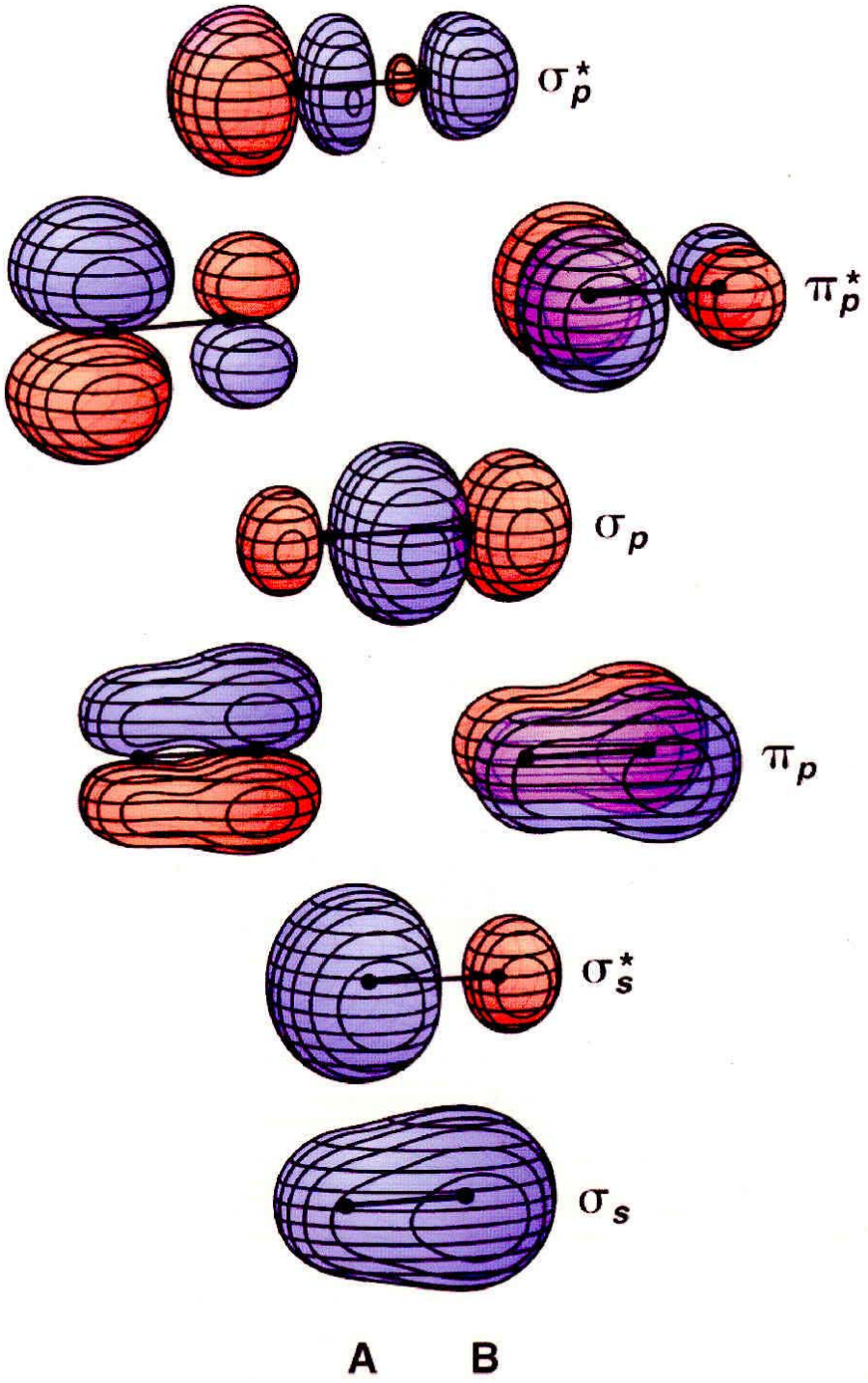

Figure 7.12
MO boundary surfaces for heteronuclear diatomic molecules AB with $\chi_B > \chi_A$. These correspond to the energy levels of Figure 7.11. The bonding orbitals are lopsided in favor of B, the antibonding in favor of A.

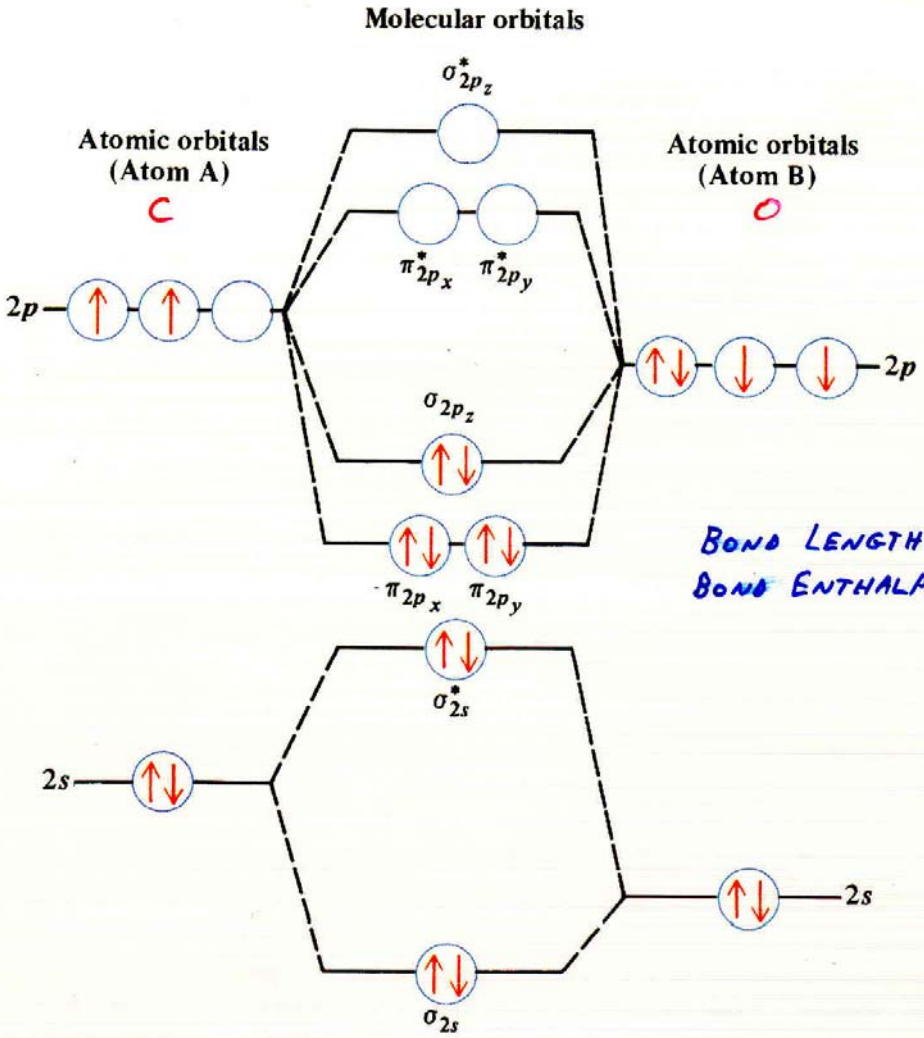

BOND LENGTH = 1.131 Å

BOND ENTHALPY = 1076 kJ/m

Figure 15-8

Correlation diagram for heteronuclear diatomic molecules, AB. The atomic orbitals for the more electronegative atom (B) are displaced downward because they have lower energies than those of A. The orbital filling shown is that for CO.

BOND ORDER = $\frac{1}{2}(8-2) = 3$

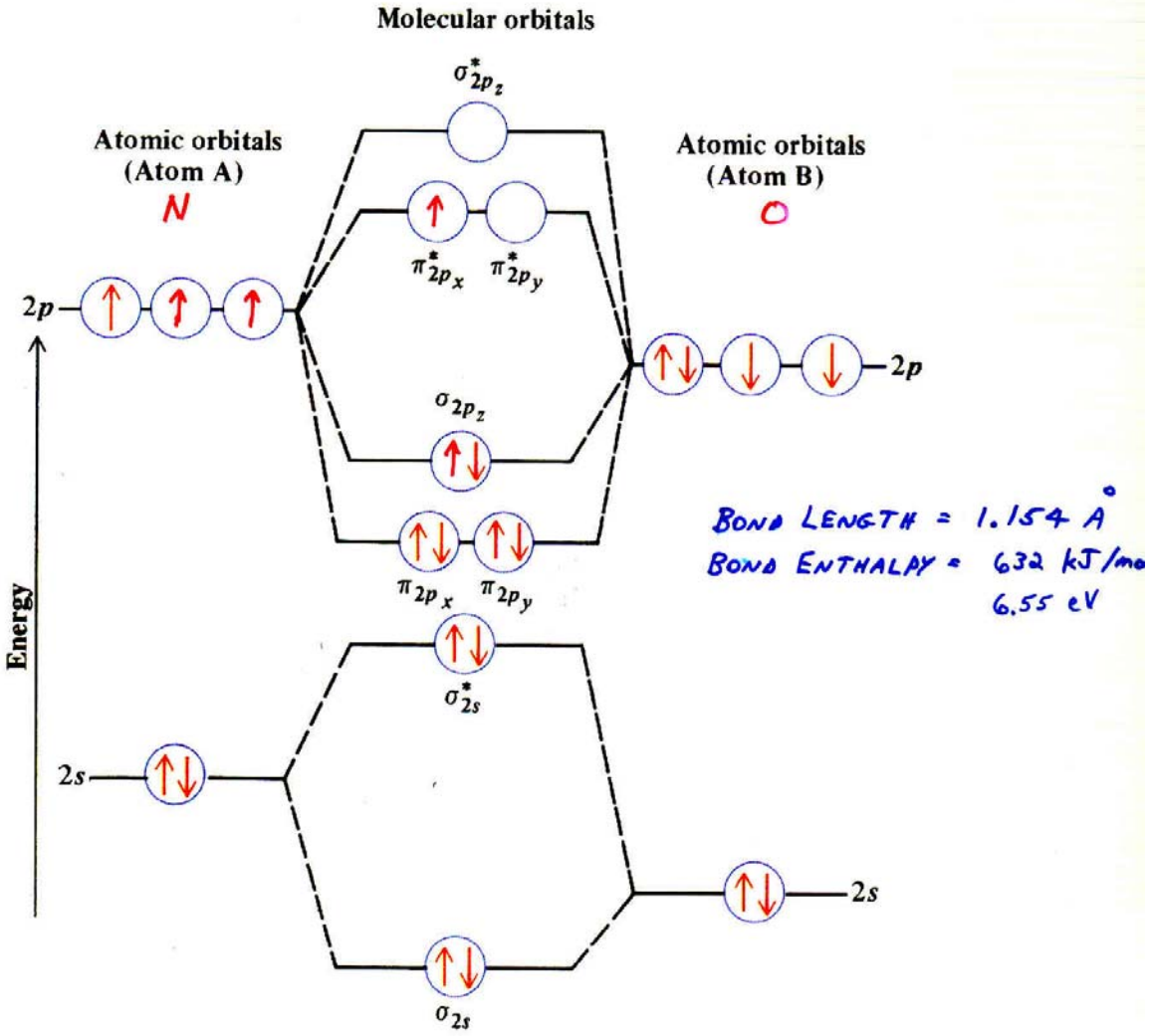

BOND LENGTH = 1.154 Å
BOND ENTHALPY = 632 kJ/mol
6.55 eV

Figure 14-18

Correlation diagram for heteronuclear diatomic molecules, AB. The atomic orbitals for the more electronegative atom (B) are displaced downward because they have lower energies than those for A. The orbital filling shown is that for NO.

BOND ORDER = $\frac{1}{2}(8-3) = 2.5$

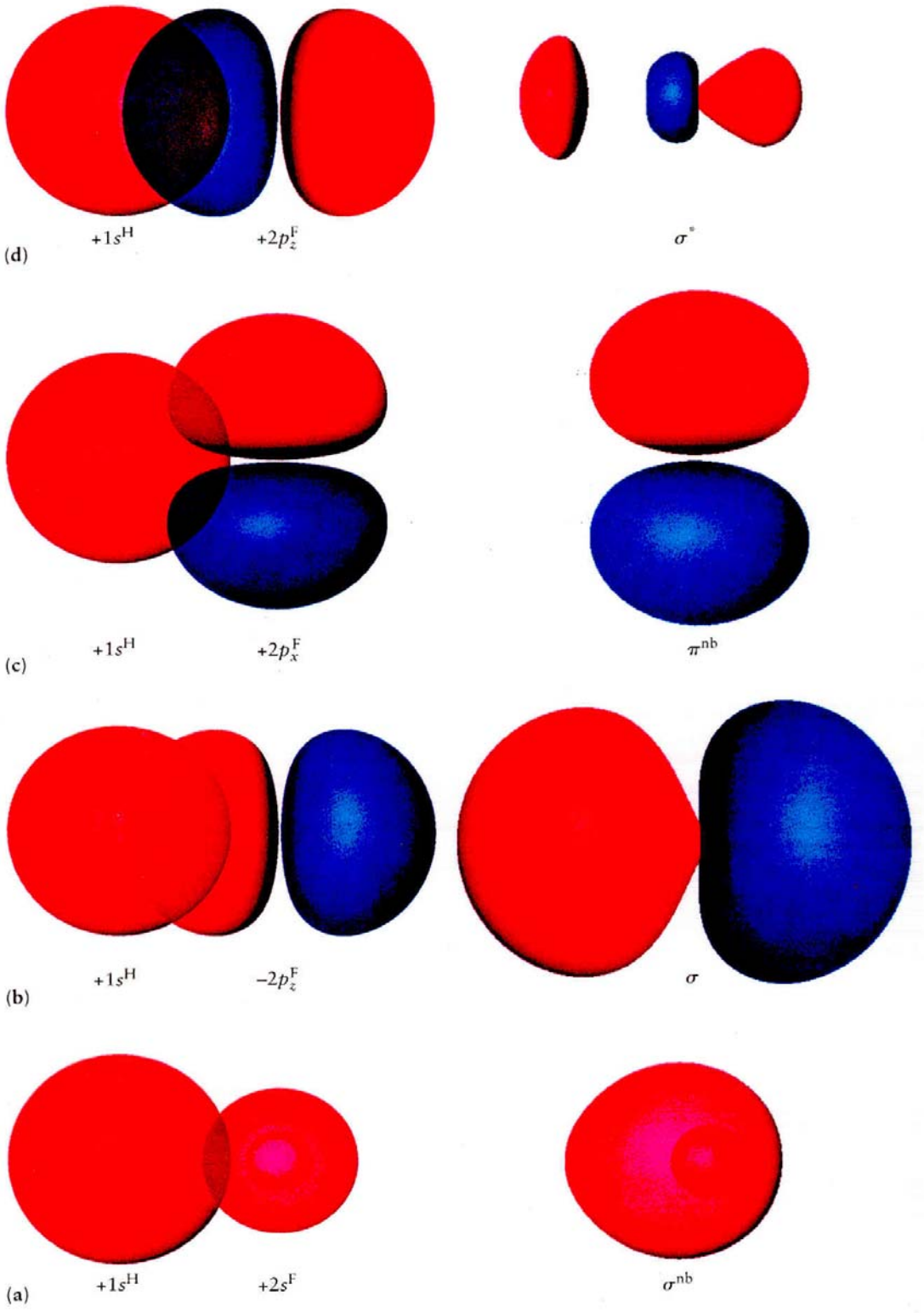

FIGURE 6.20 Overlap of atomic orbitals in HF.

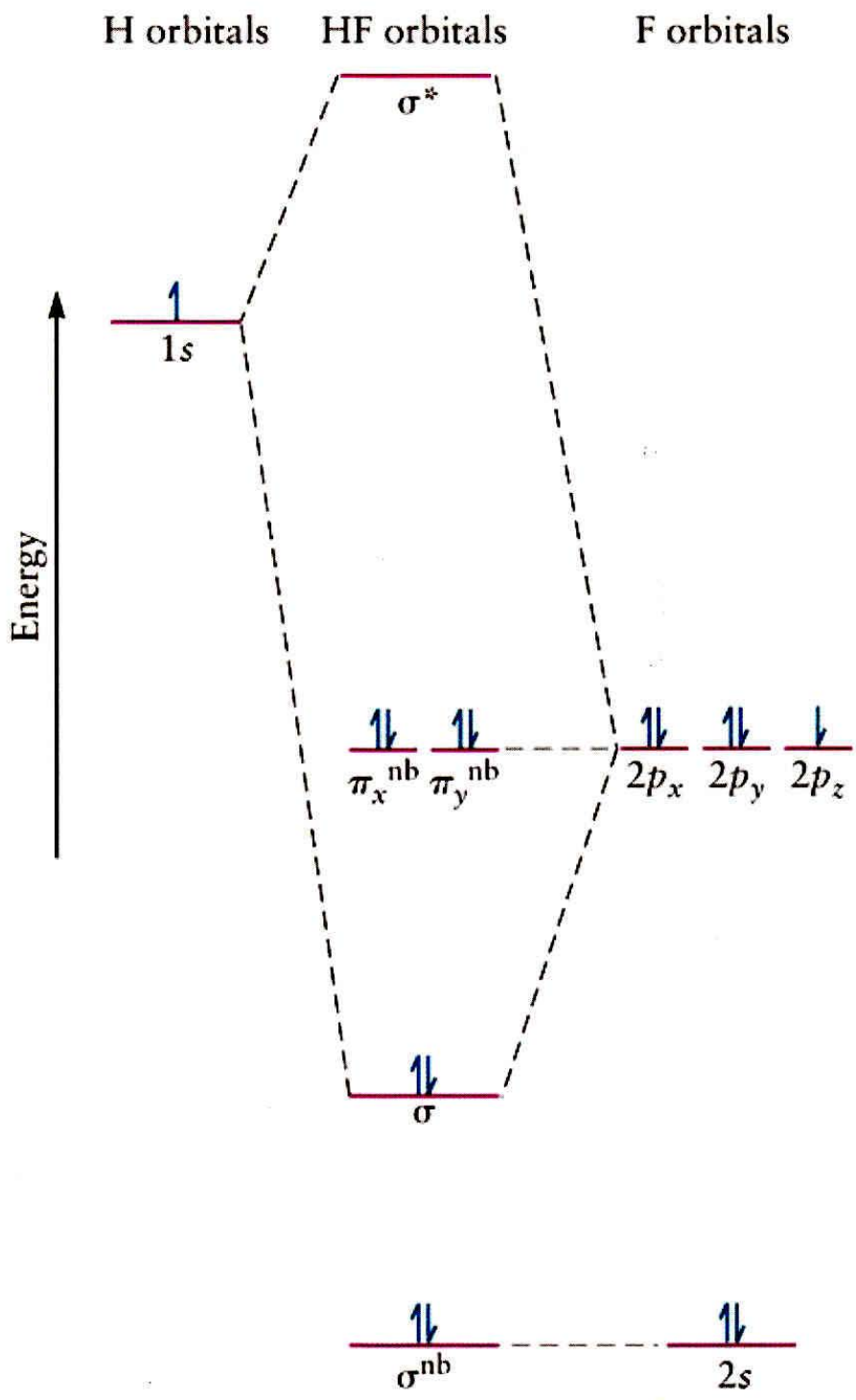

FIGURE 6.21 Correlation diagram for HF. The 2*s*, $2p_x$ and $2p_y$ atomic orbitals of fluorine do not mix with the 1*s* atomic orbital of hydrogen, and therefore remain nonbonding.

Figure 8.11: A Photoelectron Spectrometer

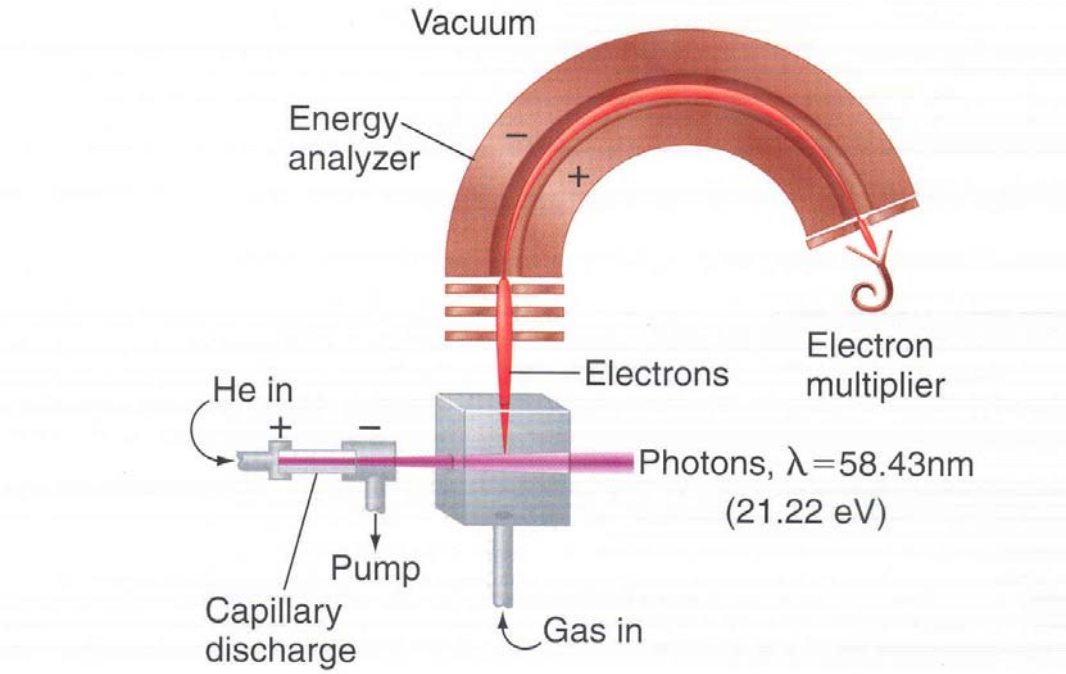

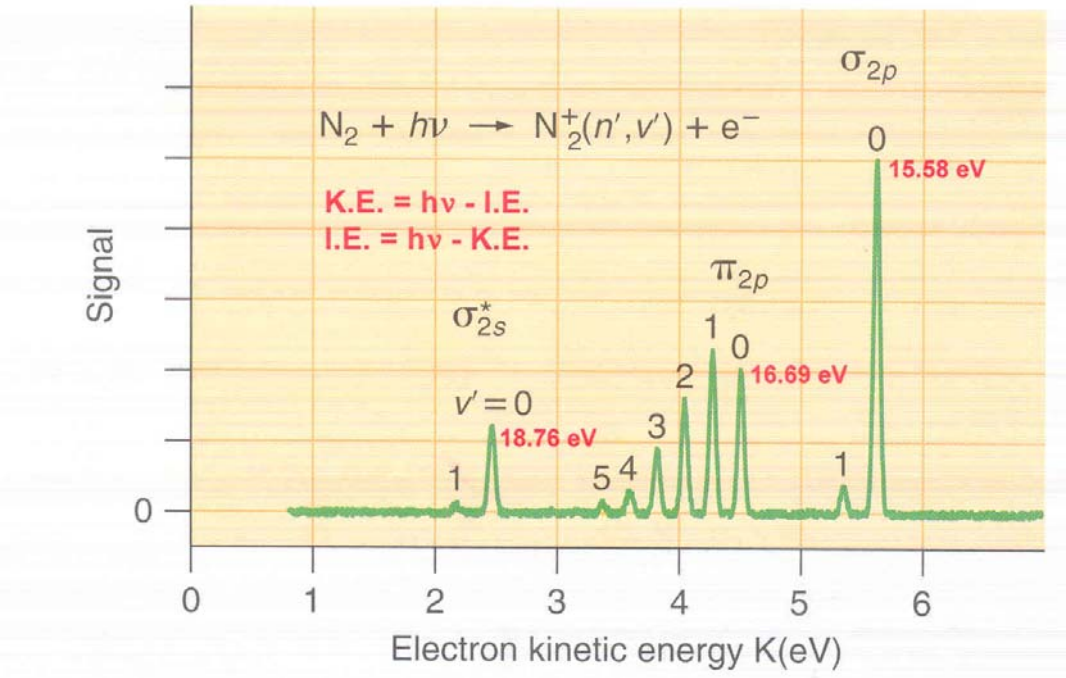

PES of N_2:

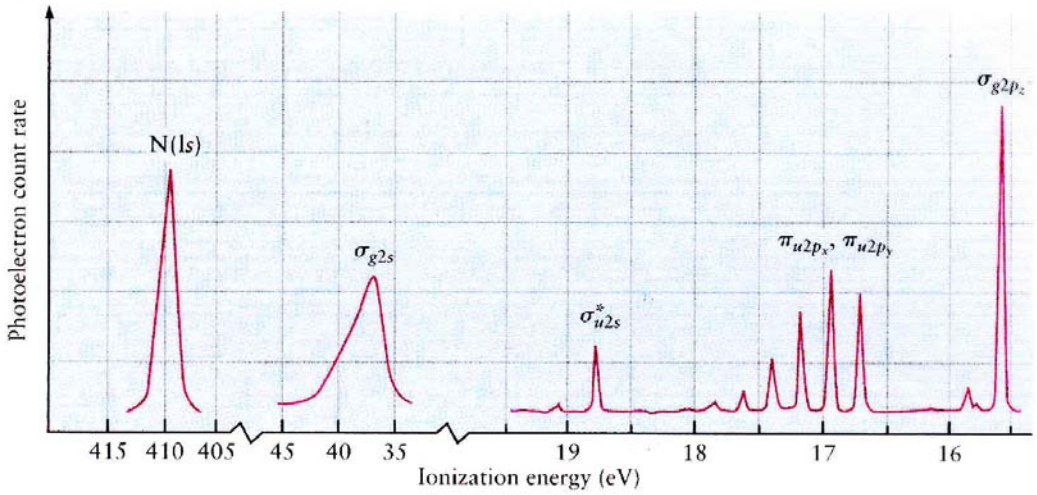

PES of O_2:

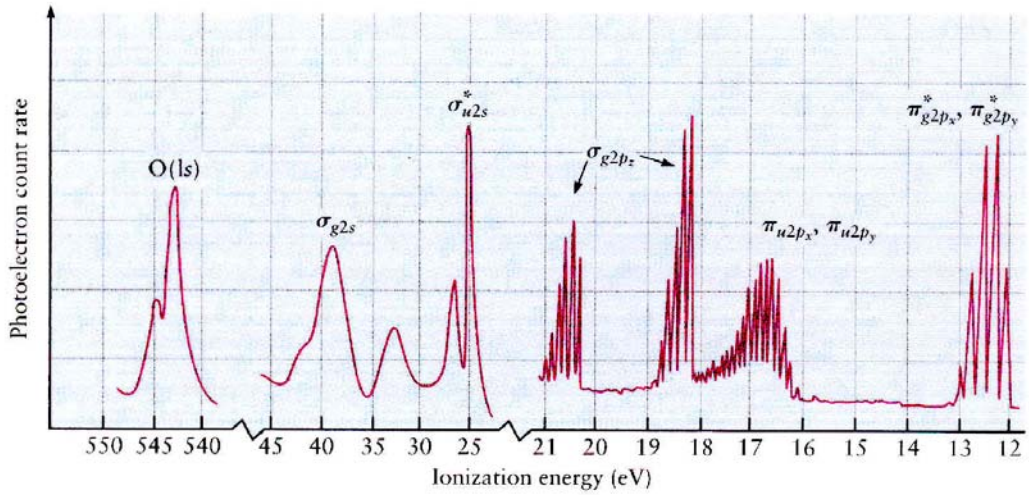

PES of NO:

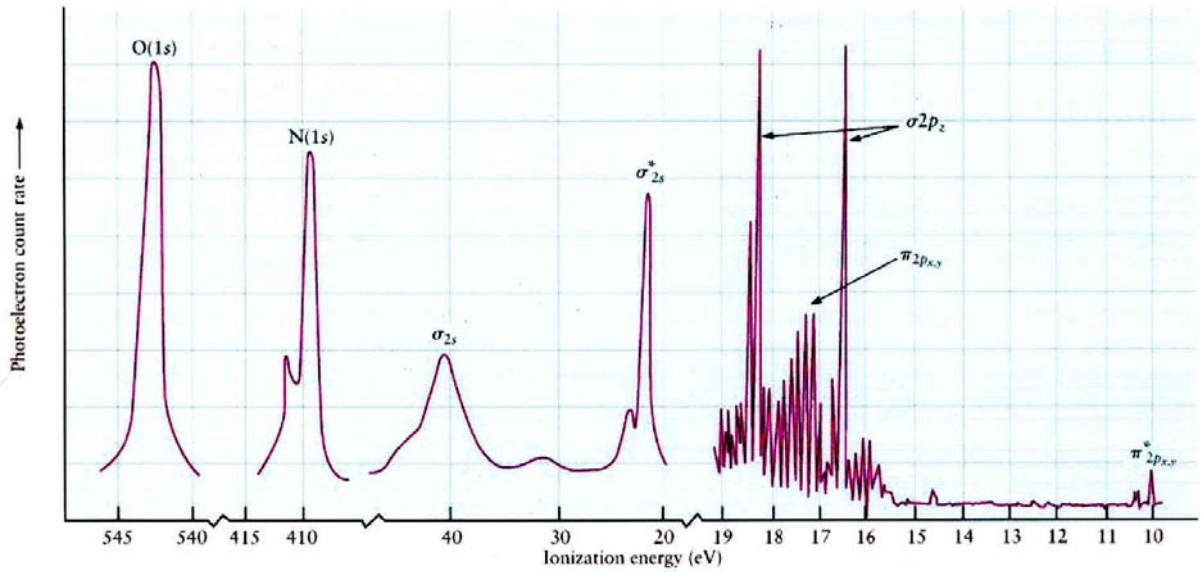

FIGURE 6.35 The photoelectron spectrum for NO. Note that the O(1s) and N(1s) orbitals remain at the same energies as in O_2 and N_2; these core electrons do not participate significantly in formation of the N−O bond. More advanced theory is required to explain why σ_{2p_z} is split into two groups.

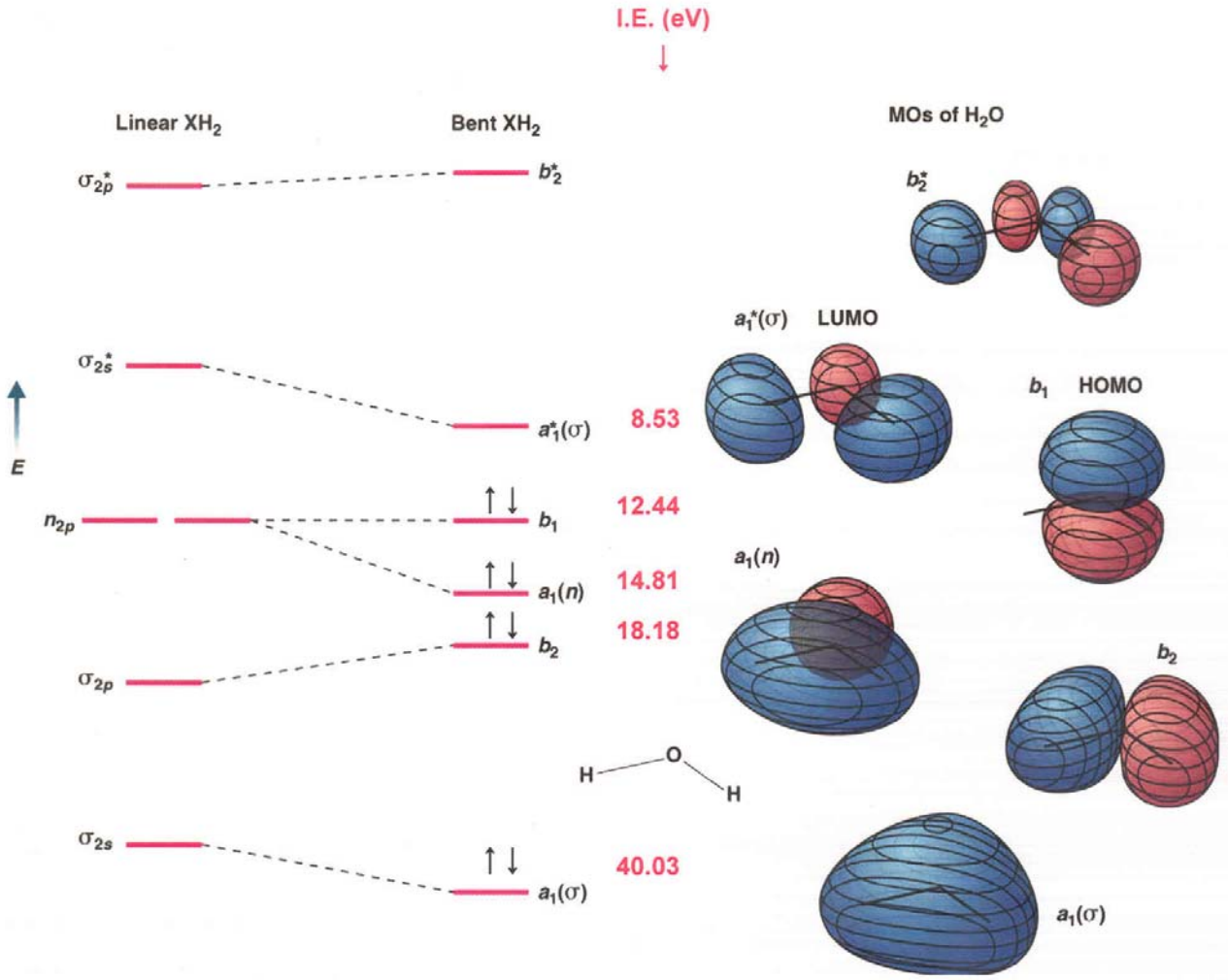

Figure 7.17
Molecular orbitals of the water molecule. Illustrated at the left is the change in energy of the various XH_2 energy levels of Figure 7.16 when the molecule is allowed to bend. The new MO labels a_1, b_1, and b_2 are necessary because the bent molecule is no longer cylindrically symmetric. The lowest four MOs on the right are occupied by electron pairs in H_2O. The most notable change from the linear case is in the $a_1(n)$ MO, which acquires some bonding character.

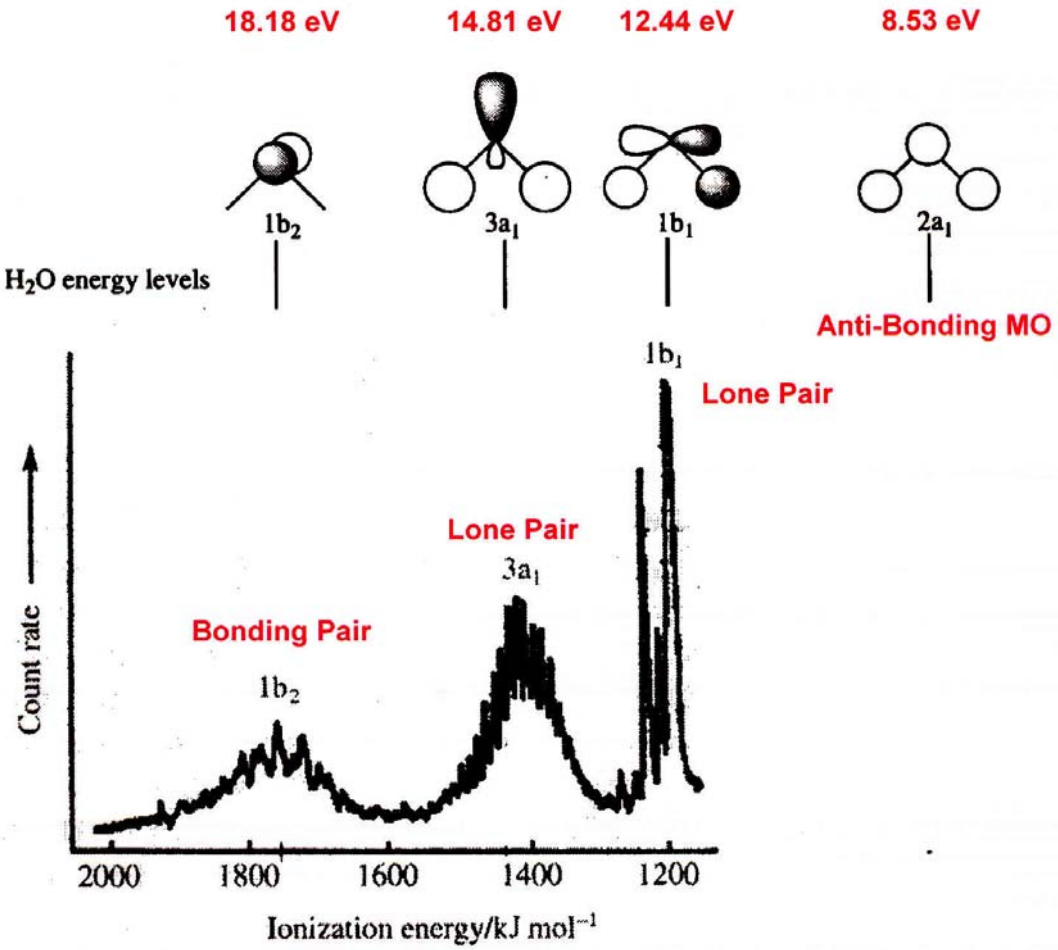

Figure 12 Photoelectron spectrum of water vapour.[1]

Figure 7.19: Delocalized π Bonding

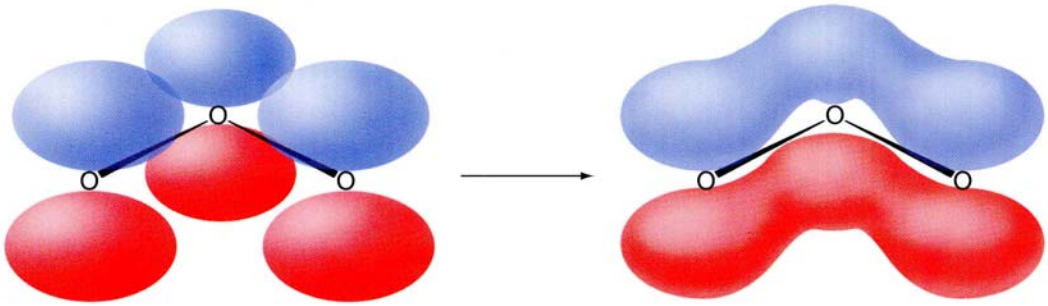

According to the Valence Bond model, π bonding in the CO_3^{2-} ion is explained by the following resonance structures:

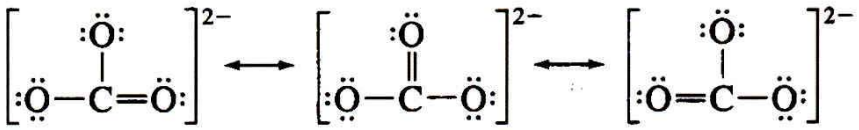

According to the Molecular Orbital model, one pair of non-bonding electrons forms a <u>delocalized</u> π bond among all four atoms of the ion:

EXAMPLE 7.5

In Example 5.2 you examined the resonance forms of the carbonate ion CO_3^{2-}. Now interpret the experimentally observed symmetrical trigonal planar structure of CO_3^{2-} with the delocalized π MO picture.

Solution:

In this case all four atoms will have *p* orbitals perpendicular to the molecular plane, and the delocalization principle dictates that the π bond MO should consist of a simultaneous constructive overlap of all three O 2*p*'s with the C 2*p*, as shown here:

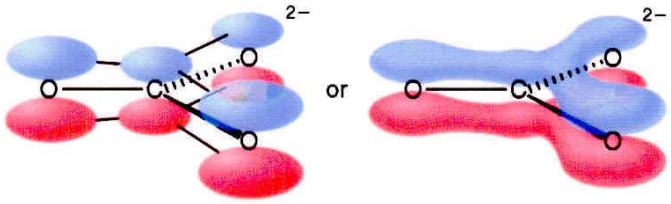

How many π MO's ?

One-third of the π bond then binds each CO pair together, leading to the observed symmetrical structure.

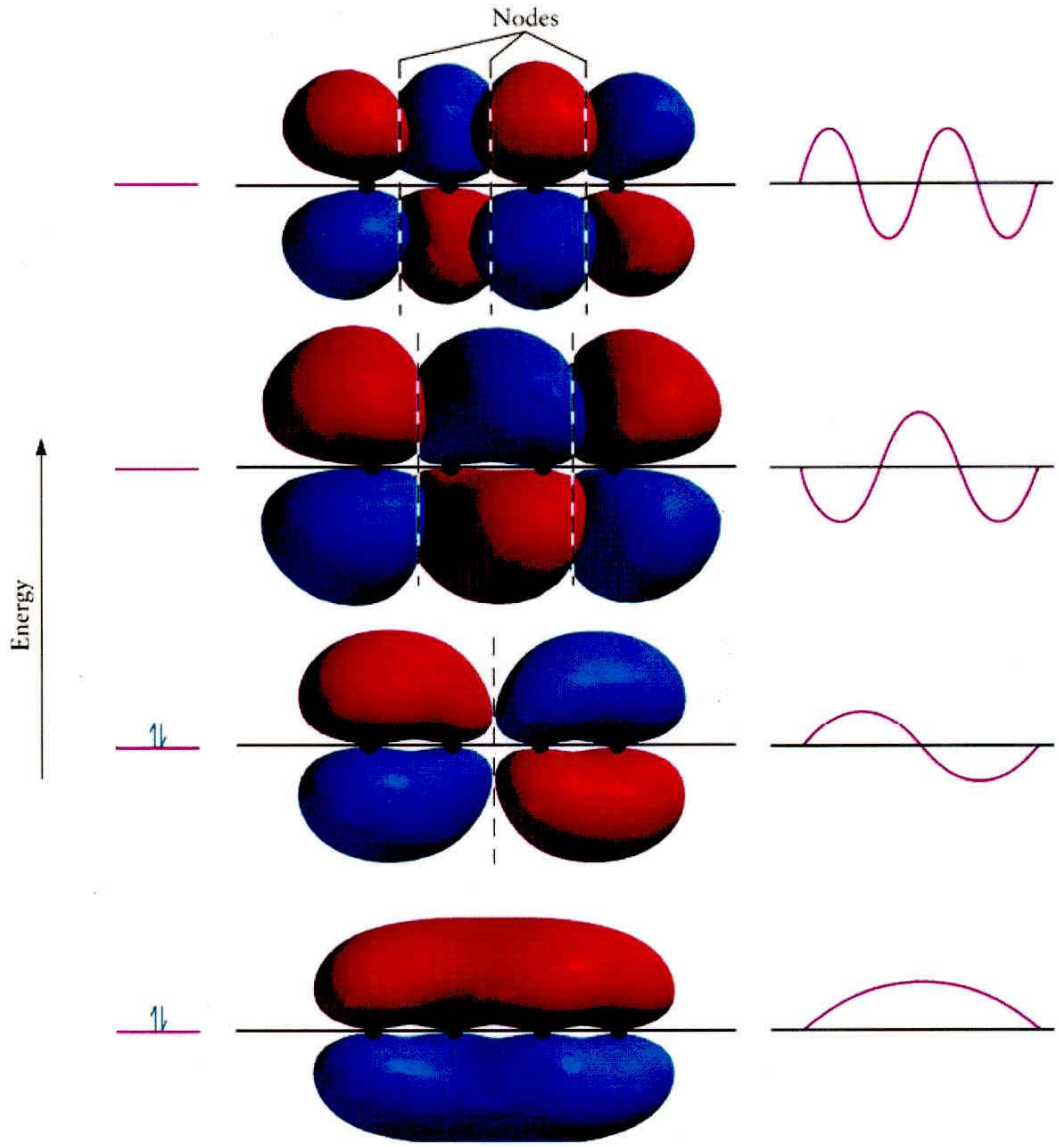

FIGURE 7.17 The four π molecular orbitals formed from four $2p_z$ atomic orbitals in 1,3-butadiene, viewed from the side. The dashed white lines represent nodes between the carbon atoms in the *y*-*z* plane. The horizontal black line represents the *x*-*y* nodal plane across which the *p* orbitals change sign. Note the similarity in the *y*-*z* nodal patterns to those of the first four modes of a vibrating string or the first four wave functions of the one-dimensional particle in a box (right). Only the lowest two orbitals are occupied in the ground state of 1,3-butadiene.

π Molecular Orbitals of 1,3-Butadiene

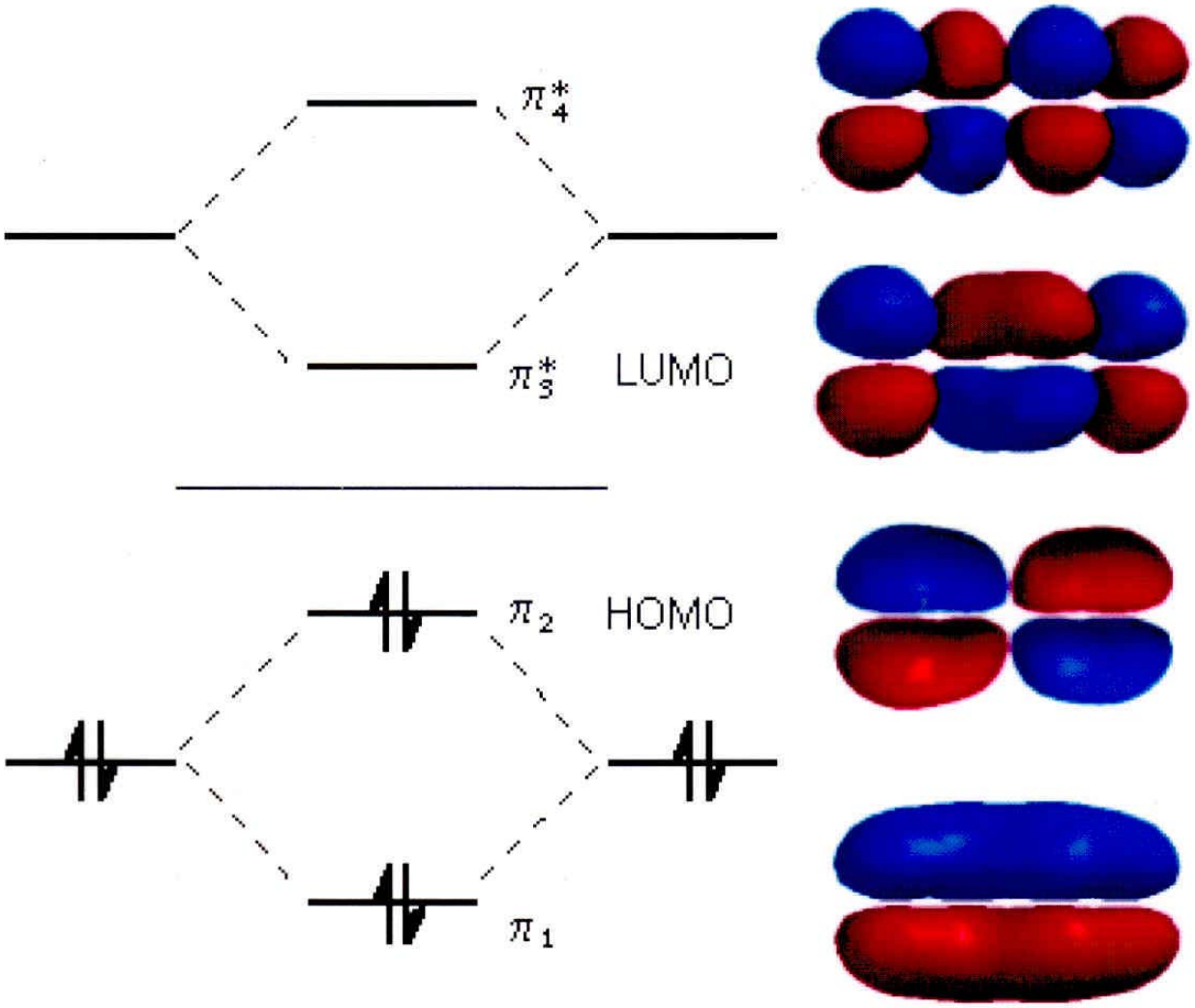

Figure 7.20: Delocalized π Bonding in Benzene

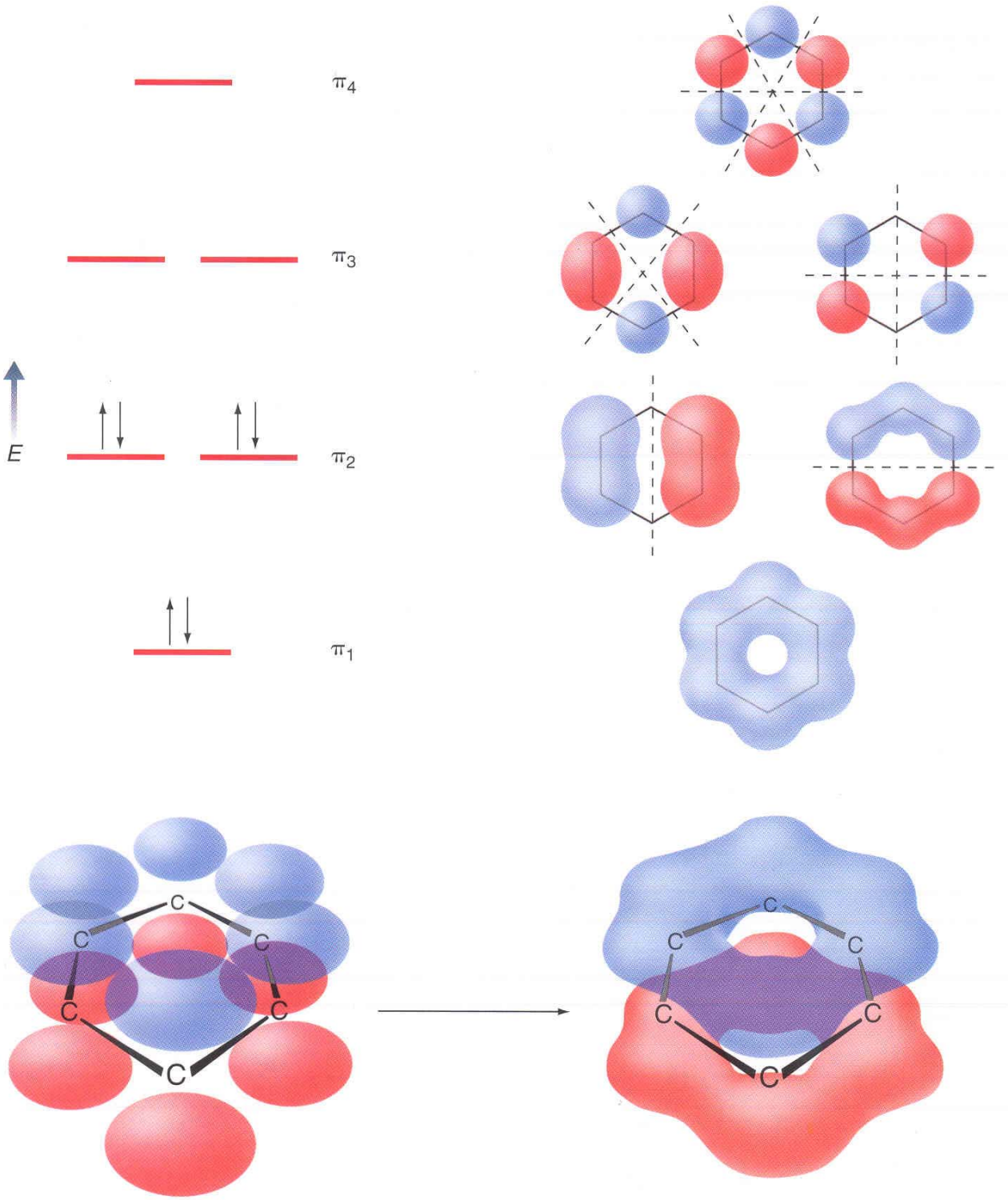

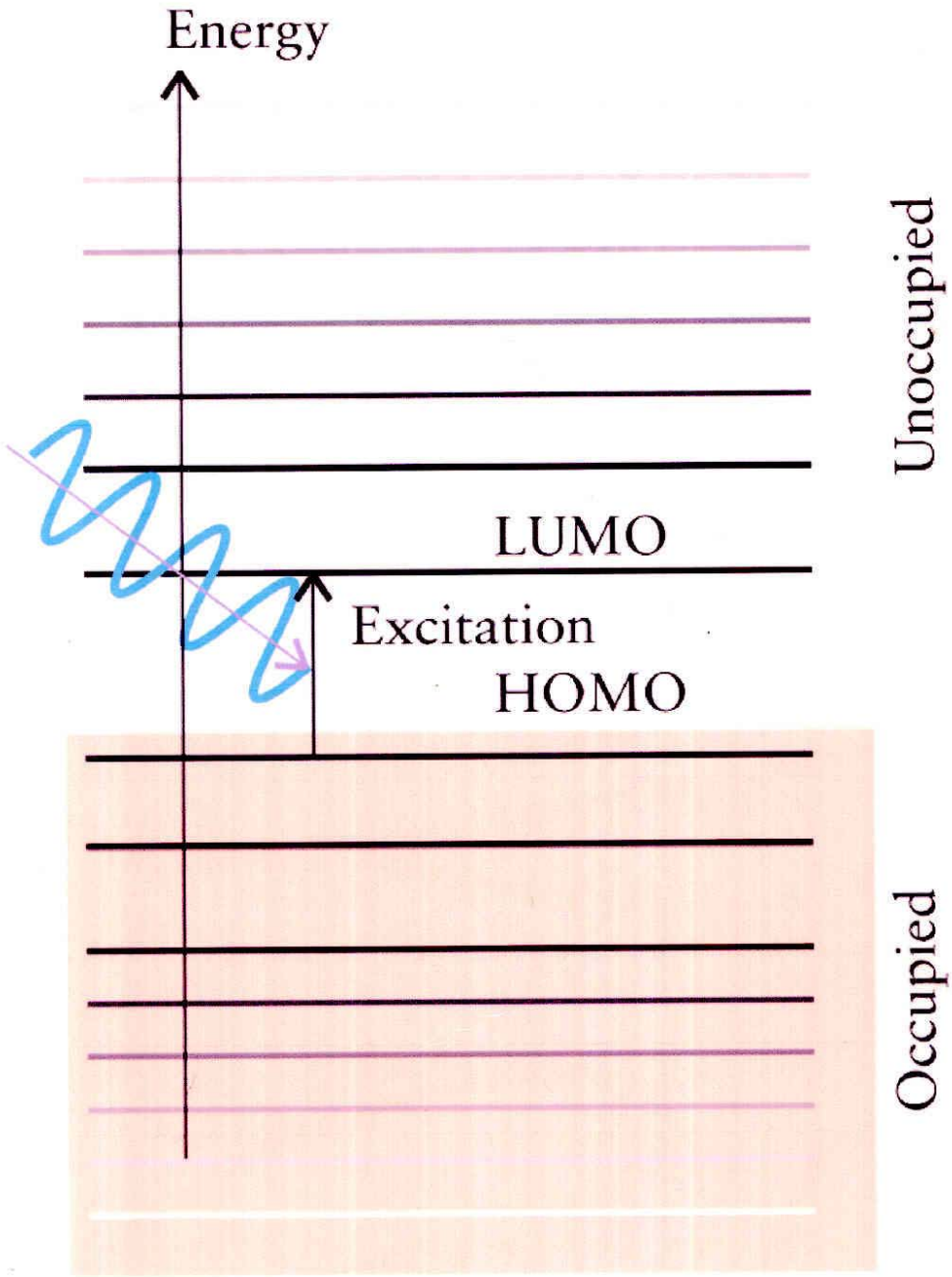

FIGURE 3.41 In large molecules, there are many closely spaced energy levels and the HOMO–LUMO gap is quite small. Such molecules are often colored because photons of visible light can be absorbed when electrons are excited from the HOMO to the LUMO.

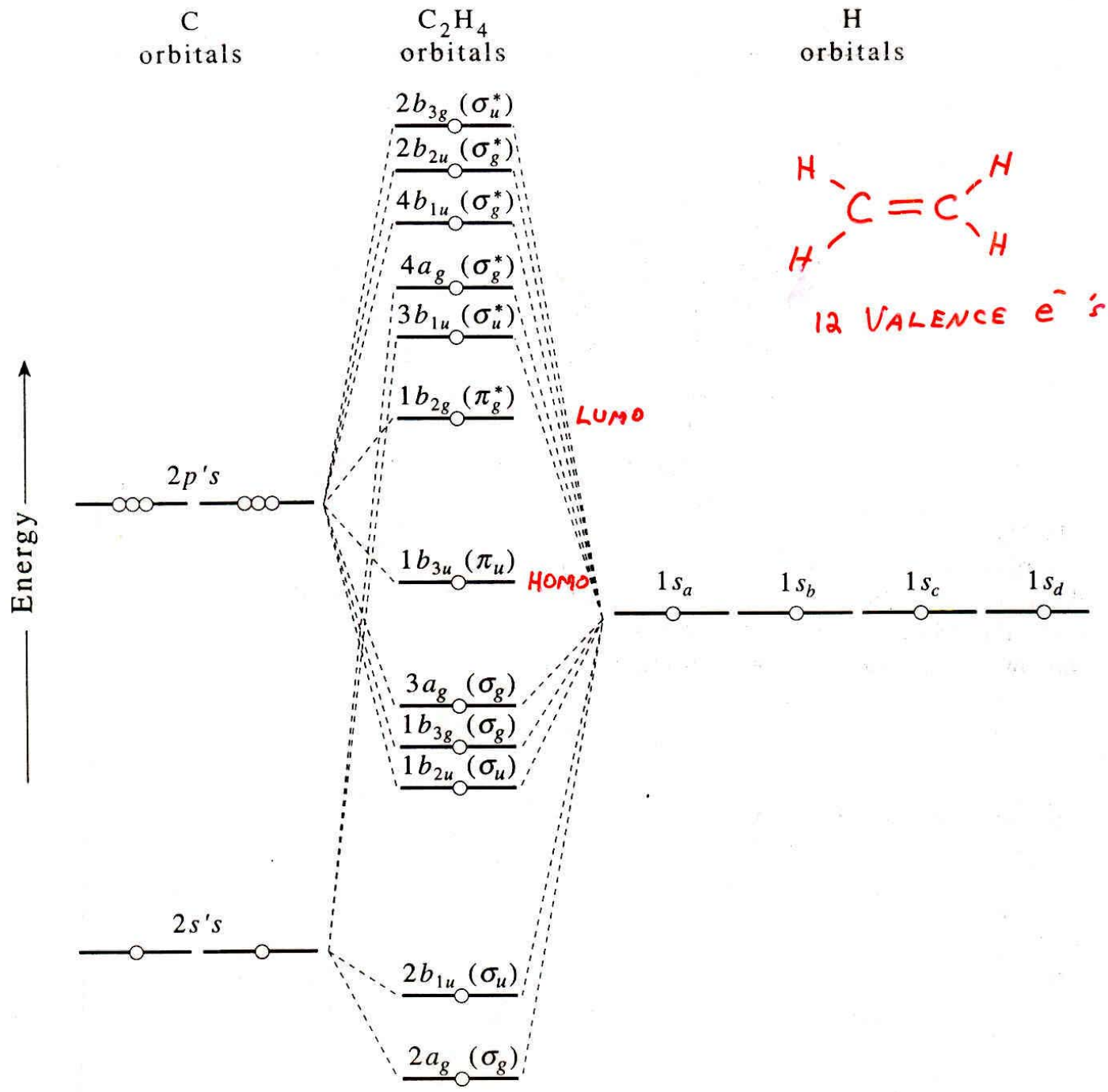

FIGURE 10.17
A molecular-orbital energy-level diagram for C_2H_4. The first five orbitals are σ orbitals, the sixth is a π orbital, the next is a π^* orbital, and the remaining five are σ^* orbitals.

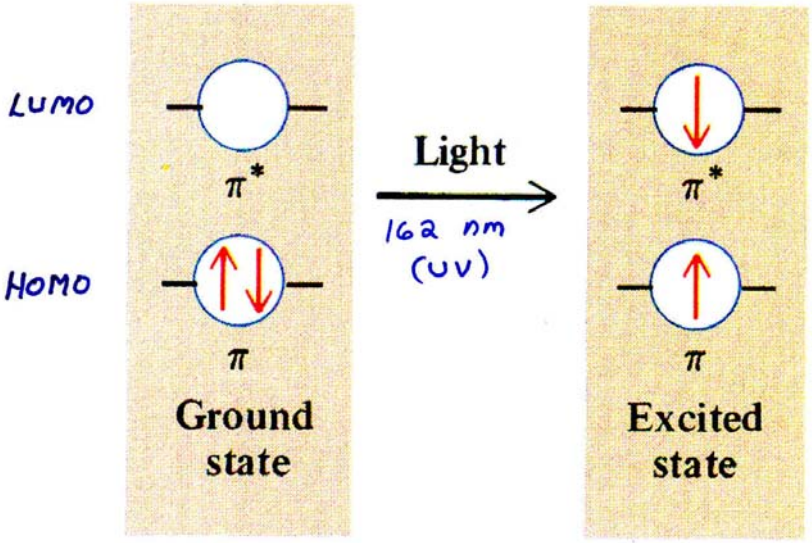

Figure 15-6

Occupancy of the π molecular orbitals in the ground state and first excited state of ethylene, C_2H_4. Ethylene in the excited state is produced by irradiation of ground-state ethylene with ultraviolet light in the appropriate frequency range.

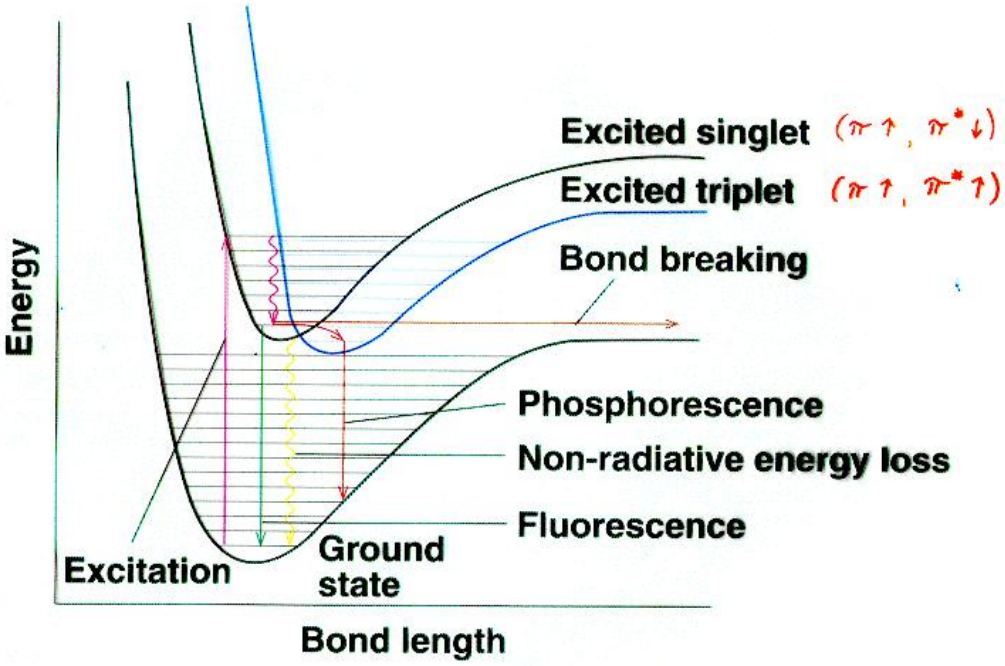

Table 15-2 Absorption of Light by Molecules with Conjugated π Electron Systems

Molecule		Number of C=C Bonds	Wavelength of Maximum Absorption (nm)
C_2H_4	C=C	1	162
C_4H_6	C=C-C=C	2	217
C_6H_8	C=C-C=C-C=C	3	251
C_8H_{10}	C=C-C=C-C=C-C=C	4	304

β-CAROTENE

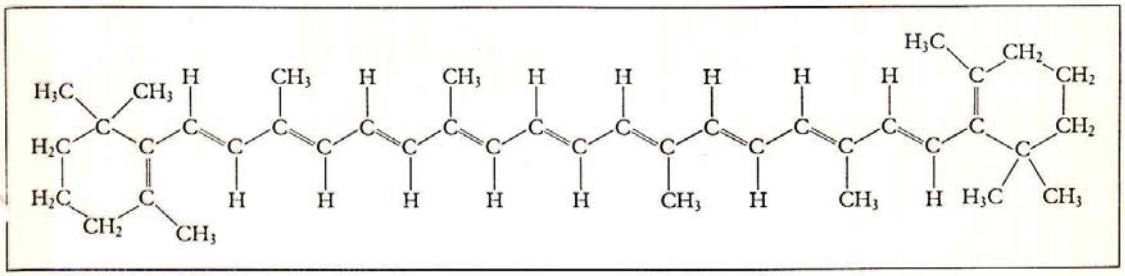

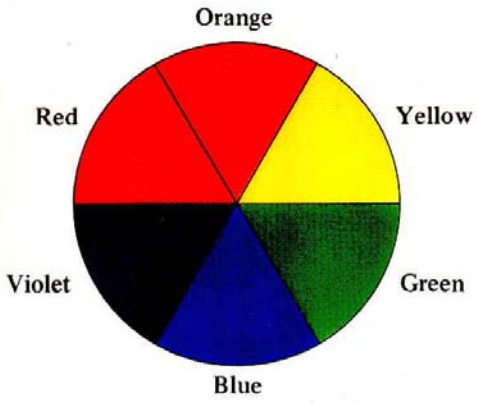

(a)

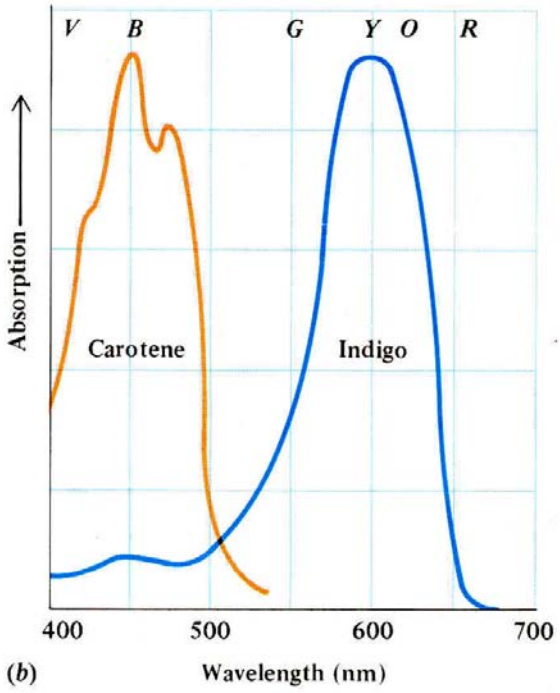

(b)

Electronic Spectrum of O_2:

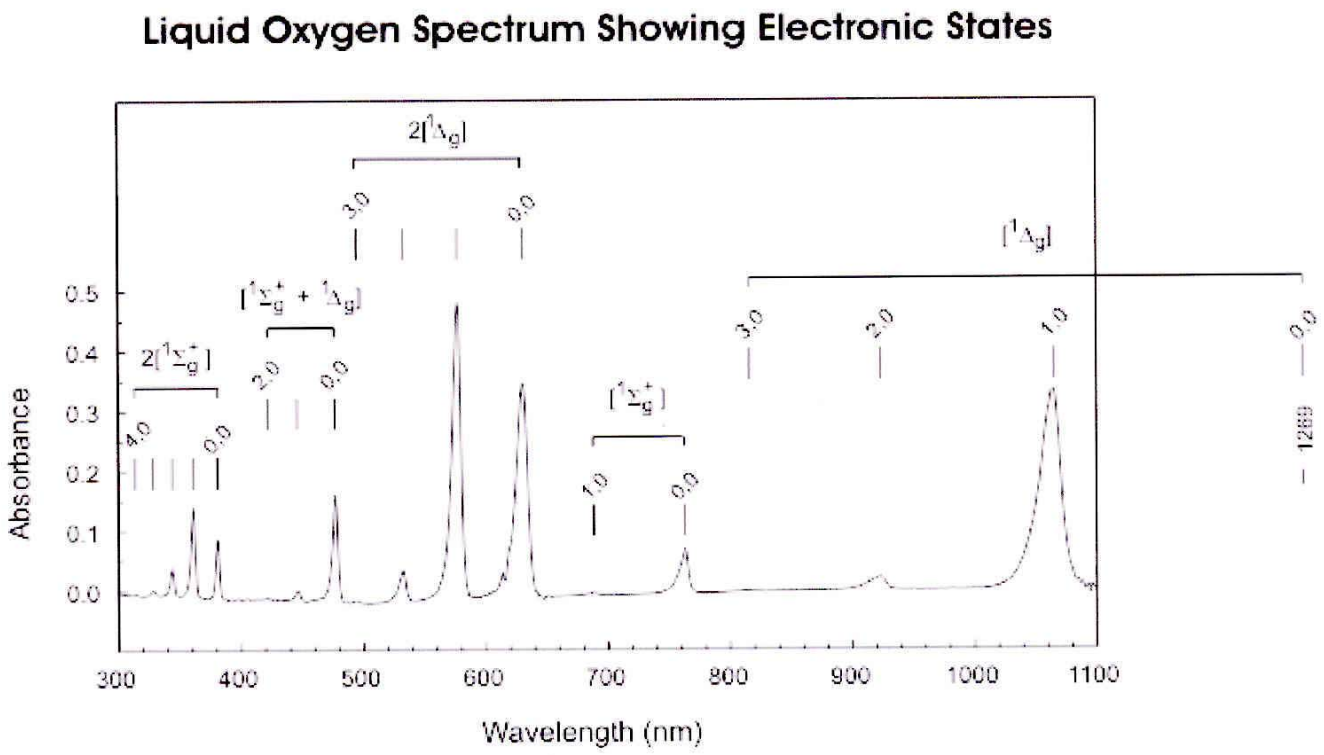

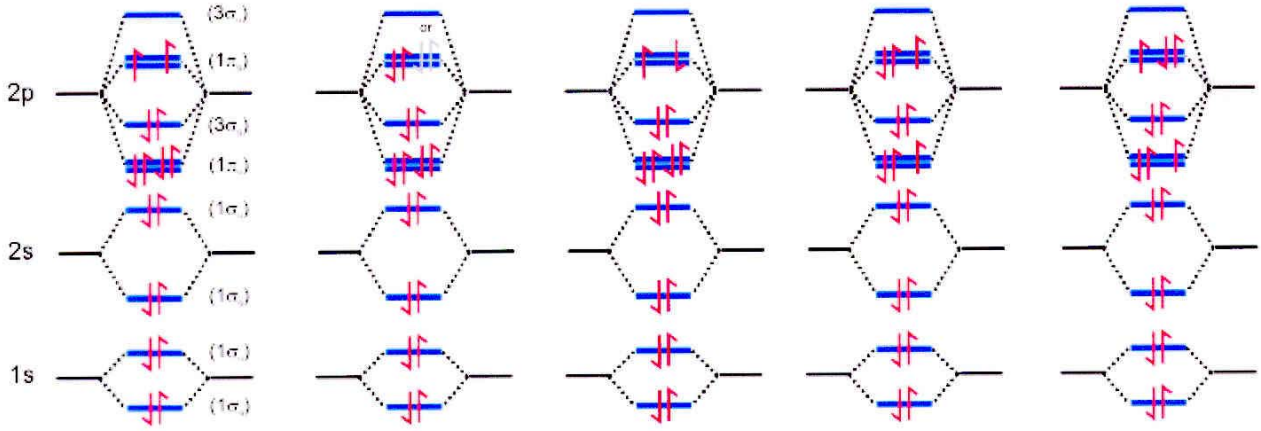

Ground State	Excited State	Excited State	Excited State	Excited State
$(^3\Sigma_g^-)$	$(^1\Delta_g)$	$(^1\Sigma_g^+)$	$(^3\Sigma_u^+)$	$(^3\Sigma_u^-)$
0 eV	1268 nm	762 nm	280 nm	202 nm
	(0.9772 eV)	(1.6266 eV)	(4.4278 eV)	(6.1202 eV)